

**Technical Paper by J.P. Giroud, T. Pelte and
R.J. Bathurst**

UPLIFT OF GEOMEMBRANES BY WIND

ABSTRACT: This paper summarizes experimental data on uplift of geomembranes by wind and presents a method to determine: the maximum wind velocity that an exposed geomembrane can withstand without being uplifted; the required thickness of a protective layer placed on the geomembrane that would prevent it from being uplifted; the tension and strain induced in the geomembrane to verify that they are below the allowable tension and strain of the geomembrane; and the geometry of the uplifted geomembrane. The method is presented in a way that should be convenient to design engineers, using equations, tables, graphical methods, and design examples. The study shows that all geomembranes can be uplifted by high velocity winds. However, the threshold wind velocity for geomembrane uplift is greater for a heavy geomembrane than for a light geomembrane. When a geomembrane is uplifted, its tension, strain and geometry depend on the wind velocity, the altitude above sea level, the location of the geomembrane in the facility (e.g. crest, slope, bottom), and the tensile characteristics of the geomembrane. As temperature influences tensile characteristics, its influence on geomembrane uplift is discussed in detail. Finally, practical recommendations are made to prevent the wind from uplifting geomembranes, or to minimize the magnitude of geomembrane uplift by the wind.

KEYWORDS: Geomembrane, Wind, Uplift, Design method.

AUTHORS: J.P. Giroud, Senior Principal, and T. Pelte, Staff Engineer, GeoSyntec Consultants, 621 N.W. 53rd Street, Suite 650, Boca Raton, Florida 33487, USA, Telephone: 1/407-995-0900, Telefax: 1/407-995-0925, and R.J. Bathurst, Professor, Department of Civil Engineering, Royal Military College of Canada, Kingston, Ontario, K7K 5L0, Canada, Telephone: 1/613-541-6000, ext. 6479, Telefax: 1/613-541-6599, E-mail: bathurst@rmc.ca.

PUBLICATION: *Geosynthetics International* is published by the Industrial Fabrics Association International, 345 Cedar St., Suite 800, St. Paul, Minnesota 55101, USA, Telephone: 1/612-222-2508, Telefax: 1/612-222-8215. *Geosynthetics International* is registered under ISSN 1072-6349.

DATES: Original manuscript received 7 July 1995, revised manuscript received 9 September 1995 and accepted 10 October 1995. Discussion open until 1 July 1996.

REFERENCE: Giroud, J.P., Pelte, T. and Bathurst, R.J., 1995, "Uplift of Geomembranes by Wind", *Geosynthetics International*, Vol. 2, No. 6, pp. 897-952.

1 INTRODUCTION

It has been observed many times that exposed geomembranes can be uplifted by the wind. Typical examples are shown in Figure 1. Generally, uplift does not cause any damage to the geomembrane or the earth structure lined with the geomembrane. However, in some cases, the geomembrane is torn, pulled out of its anchor trench, or ripped off a rigid structure to which it was connected. Also, in many cases, after uplifting has ceased, the geomembrane does not fall back exactly in the same position as before uplifting; as a result, the geomembrane is wrinkled in some areas and under tension in other areas. The senior author even knows of a case where the uplifting of the geomembrane has caused significant displacement of the underlying geotextile cushion and where it has been necessary to remove the geomembrane to reposition the geotextile. For these reasons, uplift of geomembranes by the wind is not desirable.

Geomembrane uplift can be prevented by placing a layer of heavy material such as soil, rock, or concrete on the geomembrane; a certain depth of liquid at the bottom of a pond can also prevent geomembrane uplift. This paper provides equations to determine the required thickness of the layer of heavy material, or the required depth of liquid, to prevent uplift of the geomembrane by wind. It is also shown in the paper that sandbags have a limited effectiveness.

There are, however, many cases where geomembranes are not covered with a protective layer and are, therefore, likely to be uplifted by the wind. The first question that comes to mind is: are heavy geomembranes less susceptible to uplift by wind than light geomembranes? It is shown in the paper that, indeed, at relatively small wind velocities, heavy geomembranes (such as bituminous geomembranes) are less likely to be uplifted by the wind than light geomembranes (such as some polymeric geomembranes). However, at high wind velocities, all geomembranes are likely to be uplifted and the paper provides a method for evaluating the tension, strain and deformation of a geomembrane uplifted by the wind, using estimates of wind-generated suction from wind tunnel measurements.

The equations presented in this paper are based on equations and example calculations published by the senior author in the 1970s (Giroud 1977; Giroud and Huot 1977). However, this paper contains significant new analytical developments and provides far more information than these earlier publications.

2 SUCTION CAUSED BY WIND

2.1 Reference Suction

When the wind blows, the air pressure varies locally (i.e. increases or decreases), depending on the geometry of obstacles met by the air flow. A common textbook example of the variation of air pressure over the surface of a cylinder is illustrated in Figure 2. The variation of air pressure, p_w , and wind velocity, V_w , along a stream line adjacent to the obstacle surface in Figure 2a from a reference pressure, p , and reference wind velocity, V , obeys the classical Bernoulli equation:



Figure 1. Examples of geomembrane uplift.

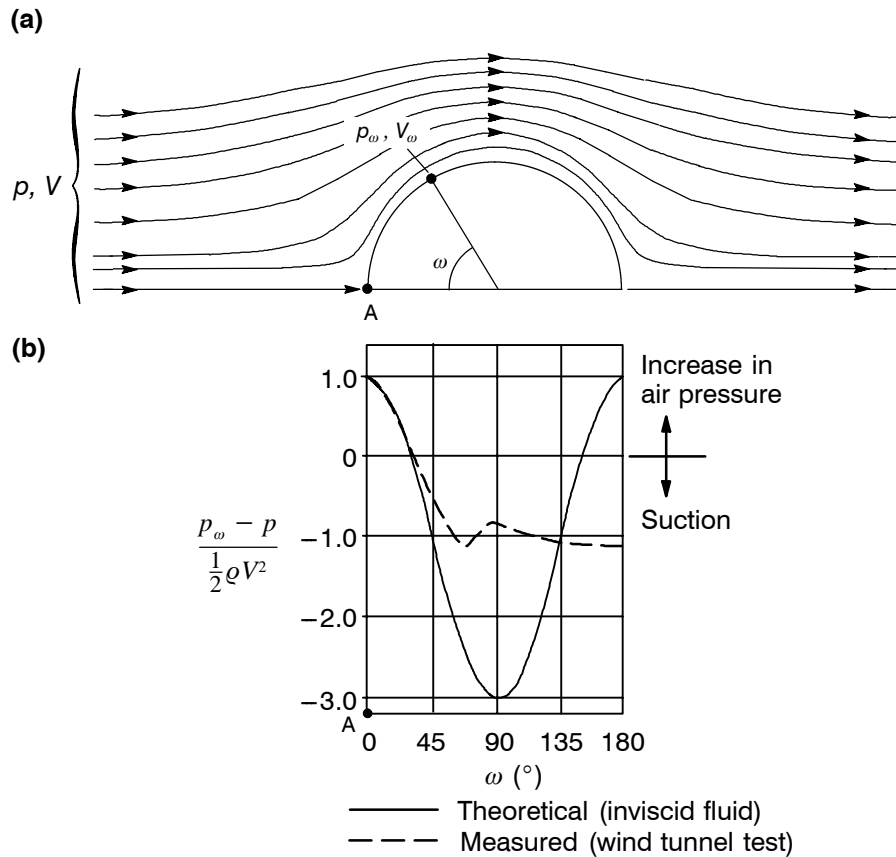


Figure 2. Illustration of pressure distribution on the surface of a cylinder (adapted from Goldstein 1938): (a) stream lines around a cylindrical obstacle; (b) air pressure variation along the surface of the obstacle.

$$p_\omega + \rho V_\omega^2/2 = p + \rho V^2/2 \quad (1)$$

where: ρ = air density. At point A, defined by $\omega = 0$ in Figure 2a, the impinging air flow strikes the cylinder at right angles and the wind velocity drops to zero at this location ($V_{(\omega=0)} = 0$). According to Equation 1 with $p_A = p_{(\omega=0)}$ and $V_{(\omega=0)} = 0$, point A is the location of maximum air pressure and, therefore, the location of maximum positive change in air pressure from the reference air pressure, p . This maximum positive change in air pressure, $\Delta p_R = p_A - p$, is both predicted by the Bernoulli equation and observed from actual air pressure measurements made on obstacles that have surfaces oriented at right angles to the direction of flow in wind tunnel tests. The maximum increase in air pressure is thus a convenient pressure change against which the distribution of air pressure at all locations along the surface of any obstacle can be referenced. This "reference

pressure variation" is obtained from the Bernoulli equation with $p_w = p_A = p + \Delta p_R$ and $V_w = 0$ and is expressed as:

$$\Delta p_R = \rho V^2 / 2 \quad (2)$$

Figure 2 also shows that potentially large negative air pressures (suctions) can develop over the surface of the cylinder. Similar, suctions can be anticipated for obstacles with geometries corresponding to berms or side slopes in geomembrane lined channels or reservoirs as demonstrated by the review of experimental data in Section 2.2.

To calculate the reference pressure variation, it is necessary to know the value of air density. Both air density and atmospheric pressure decrease as altitude above sea level increases. If isothermal conditions are assumed, the following classical equations apply:

$$\rho = \rho_o e^{-\rho_o g z / p_o} \quad (3)$$

$$p = p_o e^{-\rho_o g z / p_o} \quad (4)$$

where: ρ = air density at altitude z ; ρ_o = air density at sea level; p = atmospheric pressure at altitude z ; p_o = atmospheric pressure at sea level; g = acceleration due to gravity; and z = altitude above sea level. The atmospheric pressure at sea level under normal conditions is $p_o = 101,325$ Pa. Under that pressure, the density of dry air at sea level, at 0°C , is $\rho_o = 1.293$ kg/m³. The density of air decreases with increasing humidity and increasing temperature. The influence of humidity results from the fact that water vapor is less dense than oxygen and nitrogen. The influence of temperature is discussed below.

It should be noted that the atmospheric pressure and air density are related by the following classical equation which expresses that the air pressure at altitude z is due to the weight of the air located above this level:

$$p = \int_z^\infty \rho g dz \quad (5)$$

Equations 3 and 4 were established assuming an isothermal atmosphere. In reality, mean temperature gradients in the troposphere can influence the magnitude of air density ρ in the above expressions and hence the calculated value of pressure p . The influence of temperature gradients can be accounted for by using the U.S. Standard Atmosphere (1976) model. The U.S. Standard Atmosphere model for the range of elevations applicable to practical design problems can be expressed as:

$$p = p_o \left(1 - \frac{\beta z}{\Gamma_o} \right)^{e_o g \Gamma_o / (p_o \beta)} \quad (6)$$

where: $T_o = 288.15^\circ\text{K}$ is the standard air temperature at sea level in degrees Kelvin; and $\beta = 0.00650^\circ\text{K/m}$ is the lapse rate (the rate of change of temperature with elevation). However, the difference between pressures calculated using the U.S. Standard Atmosphere model described by Equation 6 and the simpler Equation 4 for the range of practical elevations anticipated for design is within a few percent. For the sake of simplicity, the density of dry air at 0°C will be assumed and Equation 4 will be used in the theoretical developments that follow.

Combining Equations 2 and 3 gives the following expression for the reference pressure variation as a function of the wind velocity, V , and the altitude above sea level, z :

$$\Delta p_R = \rho_o(V^2/2)e^{-\rho_o g z/p_o} \quad (7)$$

For practical calculations, the following equations can be used:

- At sea level ($z = 0$):

$$\Delta p_R = 0.6465V^2 \text{ with } \Delta p_R(\text{Pa}) \text{ and } V(\text{m/s}) \quad (8)$$

$$\Delta p_R = 0.050V^2 \text{ with } \Delta p_R(\text{Pa}) \text{ and } V(\text{km/h}) \quad (9)$$

- At altitude z above sea level:

$$\Delta p_R = 0.6465V^2e^{-(1.252 \times 10^{-4})z} \text{ with } \Delta p_R(\text{Pa}) \text{ and } V(\text{m/s}) \quad (10)$$

$$\Delta p_R = 0.050V^2e^{-(1.252 \times 10^{-4})z} \text{ with } \Delta p_R(\text{Pa}) \text{ and } V(\text{km/h}) \quad (11)$$

Equations 8 to 11 were derived from Equation 7, using the values of ρ_o and p_o given above, and using $g = 9.81 \text{ m/s}^2$. Equations 7, 10 and 11, as well as all similar equations including z that are presented in this paper, can be used with negative values of z at the few locations at the surface of the earth that are below sea level.

Values of Δp_R calculated with the above equations are given in Figure 3 as a function of altitude and wind velocity. It appears in Figure 3 that the values of the reference pressure variation, Δp_R , which typically range between 0 and 3000 Pa, are much smaller than the value of the atmospheric pressure which is, according to Equation 4:

$$\begin{aligned} p_o &= 101,325 \text{ Pa at altitude } z = 0 \text{ (sea level)} \\ p &= 78,880 \text{ Pa at altitude } z = 2000 \text{ m} \\ p &= 61,408 \text{ Pa at altitude } z = 4000 \text{ m} \end{aligned}$$

However small, suction due to wind is sufficient to uplift geomembranes as shown in Section 2.3.

The reference pressure variation can also be expressed in terms of millimeters of water. Figure 3 shows that Δp_R typically ranges between 0 and 300 mm, which is significantly less than the depth of most containment facilities lined with geomembranes. The

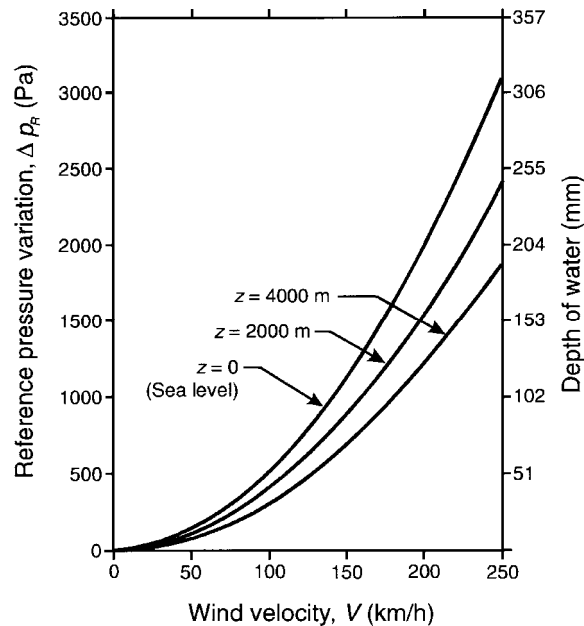


Figure 3. Reference pressure variation as a function of wind velocity and altitude above sea level.

(Note: This graph was established using Equation 11.)

required depth of water to prevent geomembrane uplift at the bottom of a reservoir will be discussed in Section 2.4, after Example 3.

2.2 Summary of Experimental Data

When the wind blows on an empty reservoir with an exposed geomembrane, some portions of the geomembrane are subjected to a suction and can be uplifted. Other portions of the geomembrane are subjected to an increased air pressure, which they should easily resist because this pressure increase is much less than the water pressure for which the geomembrane liner is designed, as mentioned above.

Wind tunnel tests were conducted by Dedrick (1973, 1974a, 1974b, 1975) for various reservoir shapes and wind directions. These tests show that, in most parts of an exposed geomembrane, the pressure variation is less than the value of the reference pressure variation, Δp_R , defined by Equation 2, and calculated using Equations 7 to 11. A summary of Dedrick's results is presented in Figure 4.

Geomembrane uplift can occur, under the conditions discussed and quantified in this paper, in areas where the wind generates a negative pressure variation ($\Delta p_R < 0$). To avoid using negative signs in most equations presented in this paper, the pressure variation, Δp , will be replaced by the suction, S , defined as follows:

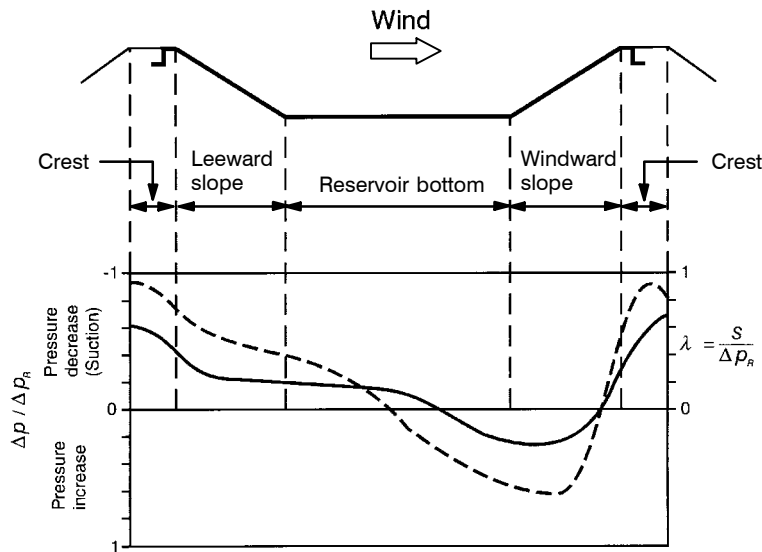


Figure 4. Change in atmospheric pressure, Δp , due to wind blowing on an empty reservoir (solid curve for wind perpendicular to dike crest line and dashed curve for worst case with wind at an angle), based on work published by Dedrick (1973, 1974a, 1974b, 1975).

(Notes: Δp_R is the reference pressure variation defined by Equation 2 and calculated using Equations 7 to 11. The axis for $\Delta p / \Delta p_R$ has been oriented downward in order to show the suction upward, which visually relates to geomembrane uplift.)

$$S = - \Delta p \quad (12)$$

The ratio between suction and reference pressure variation is the suction factor, λ , defined as follows:

$$\lambda = \frac{S}{\Delta p_R} \quad (13)$$

where Δp_R is the reference pressure variation defined by Equation 2. Only positive values of S and λ are considered herein.

Figure 4 shows that the worst case occurs when the wind blows at an angle with respect to the direction of the dikes. The following simple conclusions may be drawn from Figure 4:

- The worst situation is at the crest of the windward and leeward slopes as the wind blows across the reservoir. In this case, the maximum suction at each crest almost reaches the value of the reference pressure variation defined in Section 2.1 (i.e. the suction factor is almost $\lambda = 1.0$). However, in this case, the lower three quarters of the geomembrane-lined windward slope are subjected to a pressure increase.

- A leeward slope experiences a suction over its entire length. The suction on the leeward slope ranges between 45% of the reference pressure variation at the toe of the slope and 75% at the top of the slope, with an average value of 60%, i.e. $0.45 \leq \lambda \leq 0.75$ with an average value of 0.6.
- Large portions of the reservoir bottom are subjected to a suction ranging between 20% and 40% of the reference pressure variation ($0.2 \leq \lambda \leq 0.4$).

The above conclusions result from modeling in a wind tunnel where the wind velocity is constant. In reality, there are gusts of wind that may cause suctions greater than those indicated above, in localized areas for short periods of time.

Considering the conclusions from wind tunnel tests presented above and the need for extra safety due to gusts of wind, the following values of the suction factor, λ , are recommended for design of any slope based on the critical leeward slope:

- $\lambda = 1.00$ if the crest only is considered;
- $\lambda = 0.70$ if an entire side slope is considered;
- $\lambda = 0.85$ for the top third, $\lambda = 0.70$ for the middle third, and $\lambda = 0.55$ for the bottom third for a slope decomposed in three thirds by intermediate benches or anchor trenches as shown in Figure 7c and 7d; and
- $\lambda = 0.40$ at the bottom.

These recommendations are summarized in Figure 5. According to Equation 13, the suction factor, λ , is to be multiplied by Δp_R to obtain the suction S . The reference pressure variation, Δp_R , can be calculated using Equations 7 to 11.

It should be emphasized that the recommendations made above and used in the remainder of this paper rely entirely on the results of small-scale wind tunnel tests reported by Dedrick (1973, 1974a, 1974b, 1975). Nevertheless, the tests can be deemed representative of most practical situations because they were carried out on a wide range of dike cross section geometries and alignments typically associated with reservoir structures. However, a review of data for other shapes including obstacles with sinusoidal or smooth curve geometry can result in suction factors as great as $\lambda = 1.30$. Therefore, for unusual geometries, the designer may elect to increase the values of the suction factor, λ , given in Figure 5 by up to 30%. Also, for unusual geometries or large projects for which wind-induced damage of exposed geomembranes may have large financial consequences, wind tunnel tests of reduced-scale models or numerical simulation may be warranted.

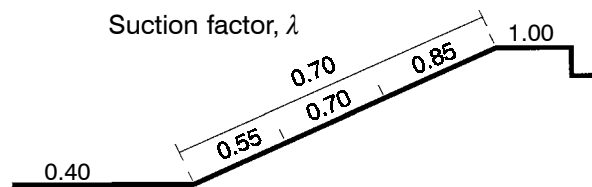


Figure 5. Recommended values of the suction factor for design of any slope based on the critical leeward slope.

2.3 Geomembrane Sensitivity to Wind Uplift

Are heavy geomembranes better able to resist wind uplift than light geomembranes? This question can be answered by comparing the weight per unit area of the geomembrane to the suction to which it is subjected, since the suction is the force per unit area that causes uplift and the weight per unit area is the force per unit area that resists uplift.

A geomembrane resists wind uplift by itself if its weight, W , per unit area, A , is greater than, or equal to, the suction to which it is subjected:

$$W/A \geq S \quad (14)$$

The weight per unit area of a geomembrane is expressed by:

$$W/A = \mu_{GM}g \quad (15)$$

where: μ_{GM} = mass per unit area of the geomembrane.

The following relationship exists between the mass per unit area of a geomembrane and its density and thickness:

$$\mu_{GM} = \rho_{GM} t_{GM} \quad (16)$$

where: ρ_{GM} = density of the geomembrane; and t_{GM} = thickness of the geomembrane. Typical values of geomembrane mass per unit area, density and thickness are given in Table 1.

Combining Equations 7, 13, 14 and 15 gives the mass per unit area of geomembrane required to resist uplift by a wind of velocity V at altitude z above sea level:

$$\mu_{GM} \geq \mu_{GMreq} = \lambda \frac{\rho_o V^2}{2g} e^{-\rho_o g z/p_o} \quad (17)$$

Using the values of ρ_o and p_o given in Section 2.1, and using $g = 9.81 \text{ m/s}^2$, the following equations may be derived from Equation 17:

- At sea level:

$$\mu_{GM} \geq \mu_{GMreq} = 0.0659\lambda V^2 \text{ with } \mu_{GMreq} \text{ (kg/m}^2\text{) and } V \text{ (m/s)} \quad (18)$$

$$\mu_{GM} \geq \mu_{GMreq} = 0.005085\lambda V^2 \text{ with } \mu_{GMreq} \text{ (kg/m}^2\text{) and } V \text{ (km/h)} \quad (19)$$

- At altitude z above sea level:

Table 1. Typical density, thickness and mass per unit area for geomembranes, and relationship between mass per unit area and minimum uplift wind velocity.

Type of geomembrane	Geomembrane density ρ_{GM} (kg/m ³)	Geomembrane thickness t_{GM} (mm)	Geomembrane mass per unit area μ_{GM} ⁽⁴⁾ (kg/m ²)	Minimum uplift wind velocity V_{upmin} ⁽⁵⁾ (km/h)
PVC ⁽¹⁾	1250 ⁽²⁾	0.5	0.63	11.1
		1.0	1.25	15.7
HDPE ⁽¹⁾	940	1.0	0.94	13.6
		1.5	1.41	16.7
		2.0	1.88	19.2
		2.5	2.35	21.5
CSPE-R ⁽¹⁾	⁽³⁾	0.75	0.9	13.3
		0.90	1.15	15.0
		1.15	1.5	17.2
EIA-R ⁽¹⁾	⁽³⁾	0.75	1.0	14.0
		1.0	1.3	16.0
Bituminous	⁽³⁾	3	3.5	26.2
		5	6	34.3

Notes: ⁽¹⁾ PVC = polyvinyl chloride; HDPE = high density polyethylene; CSPE-R = chlorosulfonated polyethylene-reinforced (commercially known as Hypalon); and EIA-R = ethylene interpolymer alloy-reinforced (commercially known as XR5). ⁽²⁾ PVC geomembranes have densities ranging typically from 1200 to 1300 kg/m³. An average value has been used in this table. ⁽³⁾ These geomembranes consist of several plies of different materials with different densities. ⁽⁴⁾ The relationship between density, thickness and mass per unit area is expressed by Equation 16. ⁽⁵⁾ Calculated using Equation 27 which is applicable to a geomembrane located at sea level and subjected to a suction equal to the reference pressure variation. Values tabulated in the last column can be found in Figure 6 on the curve for $z = 0$.

$$\mu_{GM} \geq \mu_{GMreq} = 0.0659\lambda V^2 e^{-(1.252 \times 10^{-4})z} \text{ with } \mu_{GMreq}(\text{kg/m}^2), V(\text{m/s}) \text{ and } z(\text{m}) \quad (20)$$

$$\mu_{GM} \geq \mu_{GMreq} = 0.005085\lambda V^2 e^{-(1.252 \times 10^{-4})z} \text{ with } \mu_{GMreq}(\text{kg/m}^2), V(\text{km/h}) \text{ and } z(\text{m}) \quad (21)$$

Figure 6 gives the relationship between the geomembrane mass per unit area, μ_{GM} , and the wind velocity, V , as a function of the altitude above sea level, z , for the case $\lambda = 1$, corresponding to the case where the geomembrane is subjected to a suction equal to the reference pressure variation ($S = \Delta p_R$). Figure 6 shows that typical polymeric geomembranes, with masses per unit area ranging between 0.5 and 2 kg/m², can resist uplift at sea level by winds with velocities ranging between 10 and 20 km/h, whereas bituminous geomembranes, with masses per unit area ranging between 3.5 and 6 kg/m², can resist uplift at sea level by winds with velocities ranging between 25 and 35 km/h.

Example 1. A 1.5 mm thick HDPE geomembrane is located at the bottom of a reservoir. The altitude of the reservoir is 450 m. Would this geomembrane be uplifted by a wind with a velocity of 30 km/h?

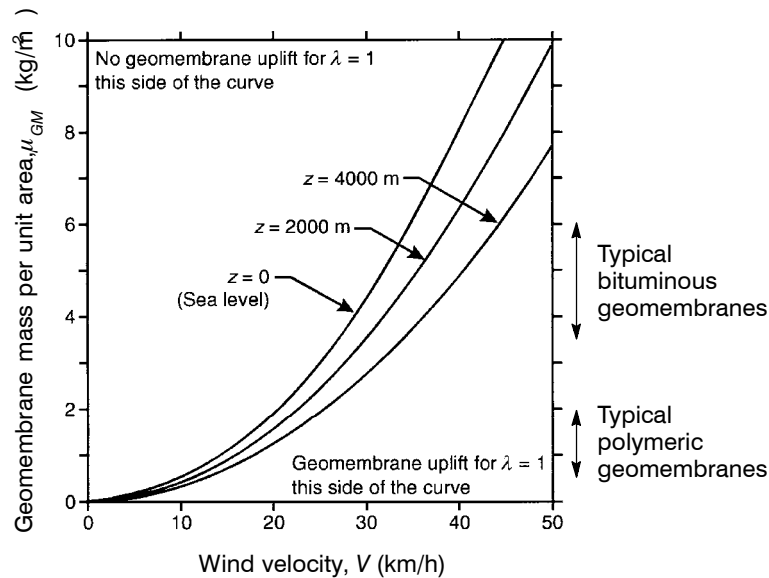


Figure 6. Relationship between geomembrane mass per unit area and wind velocity as a function of altitude above sea level ($\lambda = 1$).

(Notes: This graph can be used to determine μ_{GMreq} when V is known (see Equation 21) or V_{up} when μ_{GM} is known (see Equation 26). This graph was established using Equations 21 and 26, which are equivalent. Masses per unit area of typical geomembranes may be found in Table 1.)

As indicated in Section 2.2 and Figure 5, a value of the suction factor $\lambda = 0.4$ is recommended at the bottom of a reservoir.

Equation 21 with $\lambda = 0.4$, $V = 30$ km/h, and $z = 450$ m gives:

$$\mu_{GMreq} = (0.005085)(0.4)(30^2)e^{-(1.252 \times 10^{-4})(450)} = 1.73 \text{ kg/m}^2$$

Alternatively, Figure 6 can be used as follows. For $V = 30$ km/h the curve for $z = 0$ gives $\mu_{GM} = 4.5$ kg/m² and the curve for $z = 2000$ m gives $\mu_{GM} = 3.5$ kg/m². Interpolating between these two values gives $\mu_{GM} = 4.3$ kg/m² for $z = 450$ m. Then multiplying 4.3 kg/m² by the suction factor $\lambda = 0.4$ gives $\mu_{GMreq} = 1.72$ kg/m².

According to Table 1, the mass per unit area of a 1.5 mm thick HDPE geomembrane is 1.41 kg/m², which is less than the required value of 1.73 kg/m². Therefore, a 1.5 mm thick HDPE geomembrane would be uplifted. In contrast, a 2.0 mm thick HDPE geomembrane would not be uplifted because its mass per unit area (1.88 kg/m² according to Table 1) exceeds the value of the required mass per unit area ($\mu_{GMreq} = 1.73$ kg/m²).

END OF EXAMPLE 1

A given geomembrane (defined by its mass per unit area, μ_{GM}) should not be uplifted if the wind velocity, V , is less than a threshold wind velocity, called the uplift wind velocity, V_{up} , given by the following equation derived from Equation 17:

$$V \leq V_{up} = \left[\frac{2g\mu_{GM}}{\lambda p_o e^{-\rho_o g z / p_o}} \right]^{1/2} \quad (22)$$

Using the values of ρ_o and p_o given in Section 2.1, and using $g = 9.81 \text{ m/s}^2$, the following equations can be derived from Equation 22:

- At sea level:

$$V \leq V_{up} = 3.895 \sqrt{\mu_{GM}/\lambda} \text{ with } V_{up}(\text{m/s}) \text{ and } \mu_{GM}(\text{kg/m}^2) \quad (23)$$

$$V \leq V_{up} = 14.023 \sqrt{\mu_{GM}/\lambda} \text{ with } V_{up}(\text{km/h}) \text{ and } \mu_{GM}(\text{kg/m}^2) \quad (24)$$

- At altitude z above sea level:

$$V \leq V_{up} = 3.895 e^{(6.259 \times 10^{-5})z} \sqrt{\mu_{GM}/\lambda} \text{ with } V_{up}(\text{m/s}), z(\text{m}) \text{ and } \mu_{GM}(\text{kg/m}^2) \quad (25)$$

$$V \leq V_{up} = 14.023 e^{(6.259 \times 10^{-5})z} \sqrt{\mu_{GM}/\lambda} \text{ with } V_{up}(\text{km/h}), z(\text{m}) \text{ and } \mu_{GM}(\text{kg/m}^2) \quad (26)$$

The relationship between the wind velocity, V , and the geomembrane mass per unit area, μ_{GM} , as a function of the altitude above sea level, z , is shown in Figure 6 for a suction factor, $\lambda = 1$. The curves in Figure 6 were established using Equation 26, which is equivalent to Equation 21.

Example 2. A bituminous geomembrane with a mass per unit area of 5.5 kg/m^2 is used to line a reservoir at an altitude of 2000 m. What is the maximum wind velocity that this geomembrane can be subjected to without being uplifted?

As discussed in Section 2.2, in most usual situations, the maximum value of the suction factor is $\lambda = 1$. Using Equation 26 with $z = 2000 \text{ m}$, $\mu_{GM} = 5.5 \text{ kg/m}^2$ and $\lambda = 1$ gives:

$$V_{up} = 14.023 e^{(6.259 \times 10^{-5})(2000)} \sqrt{5.5/1} = 37.3 \text{ km/h}$$

The same value can be found in Figure 6.

END OF EXAMPLE 2

The last column of Table 1 gives minimum values of the uplift wind velocity, V_{upmin} , for typical geomembranes calculated using the following equation derived from Equation 24 with $\lambda = 1$, i.e. assuming that the geomembrane is located at sea level and that

the suction to which the geomembrane is subjected is equal to the reference pressure variation:

$$V_{upmin} = 14\sqrt{\mu_{GM}} \text{ with } V_{upmin}(\text{km/h}) \text{ and } \mu_{GM}(\text{kg/m}^2) \quad (27)$$

It should be noted that the values of uplift wind velocity given in Figure 6 and Table 1 are usually minimum values because the case considered ($\lambda = 1$) corresponds generally to maximum suction. In other words, the uplift wind velocity values given in Table 1 are the wind velocities below which a given geomembrane should not be uplifted regardless of its location in the considered facility, and it is not certain that the geomembrane will be uplifted if the wind velocity is greater than the value tabulated. For example, for a 2 mm thick HDPE geomembrane ($\mu_{GM} = 1.88 \text{ kg/m}^2$ according to Table 1), at sea level, the minimum wind uplift velocity is $V_{upmin} = 19.2 \text{ km/h}$, according to Table 1 and Figure 6. If this geomembrane is located in an area where the suction is only 45% of the reference suction, Equation 24 with $\lambda = 0.45$ gives:

$$V_{up} = 14.023\sqrt{1.88/0.45} = 28.7 \text{ km/h}$$

Under the same circumstances, but at an altitude of 1500 m, Equation 26 gives:

$$V_{up} = (14.023)e^{(6.259 \times 10^{-5})(1500)}\sqrt{1.88/0.45} = 31.5 \text{ km/h}$$

2.4 Required Uniform Pressure to Counteract Wind Uplift

Uplift of a geomembrane by the wind can be prevented by placing a layer of protective material on the geomembrane. The required depth of the protective layer, D_{req} , can be calculated by equating the pressure resulting from the weight of the protective layer plus the weight of the geomembrane to the suction exerted by the wind as follows:

$$\rho_P g D_{req} + \mu_{GM} g \geq S \quad (28)$$

where ρ_P is the density of the protective layer material.

Combining Equations 7, 13 and 28 gives:

$$D_{req} \geq \frac{1}{\rho_P} \left(-\mu_{GM} + \lambda \frac{\rho_o V^2}{2g} e^{-\rho_o g z / \rho_o} \right) \quad (29)$$

For wind velocities less than V_{up} defined by Equation 22 or, for geomembrane masses per unit area greater than μ_{GMreq} defined by Equation 17, Equation 29 gives a negative value for D_{req} , which means that, in such cases, no protective layer is required. However, in most practical cases, μ_{GM} is small compared to the term that contains V^2 in Equa-

tion 29; in other words, the wind velocity is such that a protective layer is required to prevent geomembrane uplift.

Using the values of q_o and p_o given in Section 2.1, and using $g = 9.81 \text{ m/s}^2$, the following equations may be derived from Equation 29:

- At sea level:

$$D_{req} = \frac{1}{\rho_P}(-\mu_{GM} + 0.0659\lambda V^2) \quad (30)$$

with D_{req} (m), ρ_P (kg/m^3), μ_{GM} (kg/m^2), V (m/s)

$$D_{req} = \frac{1}{\rho_P}(-\mu_{GM} + 0.005085\lambda V^2) \quad (31)$$

with D_{req} (m), ρ_P (kg/m^3), μ_{GM} (kg/m^2), V (km/h)

- At altitude z above sea level:

$$D_{req} = \frac{1}{\rho_P}(-\mu_{GM} + 0.0659\lambda V^2 e^{-(1.252 \times 10^{-4})z}) \quad (32)$$

with D_{req} (m), ρ_P (kg/m^3), μ_{GM} (kg/m^2), V (m/s), z (m)

$$D_{req} = \frac{1}{\rho_P}(-\mu_{GM} + 0.005085\lambda V^2 e^{-(1.252 \times 10^{-4})z}) \quad (33)$$

with D_{req} (m), ρ_P (kg/m^3), μ_{GM} (kg/m^2), V (km/h), z (m)

An airtight protective cover that does not adhere to the geomembrane can be uplifted independently of the geomembrane. Therefore, the wind uplift resistance of the airtight protective cover itself should be evaluated using Equations 29 to 33 from which μ_{GM} is deleted. However, this comment is mostly of academic interest since μ_{GM} is generally negligible in Equations 29 to 33, as seen in the following example.

Example 3. A 1.3 mm thick PVC geomembrane is placed on the side slope and on the crest of a reservoir at an altitude of 1700 m. The expected wind velocity is 120 km/h. What is the required thickness of a soil protective layer, with a density of 1800 kg/m^3 , at the crest of the slope?

First, the mass per unit area of the geomembrane must be calculated using Equation 16 as follows:

$$\mu_{GM} = (1250)(1.3 \times 10^{-3})$$

(where the density of the PVC geomembrane found in Table 1 is used) hence:

$$\mu_{GM} = 1.625 \text{ kg/m}^2$$

According to Figure 4, the maximum value of the suction factor, λ , at the crest of a slope is $\lambda = 1$. (See also recommended values for λ in Figure 5.)

Equation 33 with $\rho_p = 1800 \text{ kg/m}^3$, $\mu_{GM} = 1.625 \text{ kg/m}^2$, $\lambda = 1$, $V = 120 \text{ km/h}$, and $z = 1700 \text{ m}$, gives:

$$D_{req} = \frac{1}{1800} \left(-1.625 + (0.005085)(1)(120^2)e^{-(1.252 \times 10^{-4})(1700)} \right)$$

$$\text{hence: } D_{req} = \frac{1}{1800} (-1.625 + 59.186) = 0.032 \text{ m} = 32 \text{ mm}$$

It appears that the geomembrane mass per unit area, $\mu_{GM} = 1.625 \text{ kg/m}^2$, is very small compared to the term due to the wind (59.186 kg/m^2). If the geomembrane mass per unit area is neglected in the above calculations, the calculated thickness becomes 33 mm.

END OF EXAMPLE 3

The liquid stored in a reservoir acts as a protective layer for the portions of geomembrane located below the liquid level. The required depth of liquid can be calculated using Equations 29 to 33 where ρ_p is the density of the protective liquid. However, it is suggested to use a factor of safety such as 2 with these equations considering that the depth of liquid may decrease in some areas due to a phenomenon called "setdown" created by wind shear acting over the surface of the impounded liquid.

Example 4. A 0.75 mm thick CSPE-R geomembrane is used to line the bottom of a reservoir located 700 m above sea level. What minimum depth of water should be kept in the reservoir, to prevent geomembrane uplift at the bottom, at the beginning of a season when wind velocities of 160 km/h can be expected?

According to Table 1, the mass per unit area of a 0.75 mm thick CSPE geomembrane is 0.9 kg/m^2 . According to Section 2.2 and Figure 5, a recommended value for the suction factor, λ , at the bottom of the reservoir is 0.4. Using Equation 33 with $\rho_p = 1000 \text{ kg/m}^3$ (density of water), $\mu_{GM} = 0.9 \text{ kg/m}^2$, $\lambda = 0.4$, $V = 160 \text{ km/h}$, and $z = 700$ gives:

$$D_{req} = \frac{1}{1000} \left[-0.9 + (0.005085)(0.4)(160^2)e^{-(1.252 \times 10^{-4})(700)} \right]$$

$$\text{hence: } D_{req} = (-0.9 + 47.7)/1000 = 0.047 \text{ m} = 47 \text{ mm}$$

A factor of safety of 2 is recommended for the reasons indicated above. Therefore, a minimum depth of water of 94 mm should be left permanently at the bottom of the reservoir.

END OF EXAMPLE 4

Are sandbags effective? To answer this question, a simple evaluation can be made, which consists of calculating the required spacing between sandbags. Considering a typical 25 kg (~ 250 N) sandbag, and a typical suction of 1000 Pa, i.e. 1000 N/m^2 , the weight of the sandbag corresponds to that suction over an area of $250/1000 = 0.25 \text{ m}^2$, hence a required center-to-center distance of 0.5 m between sandbags. This indicates that a large number of sandbags would be required to resist wind uplift by a suction which corresponds to a wind velocity on the order of 150 km/h.

Sandbags placed 3 m apart can resist a suction of $250/9 = 28$ Pa, hence a wind velocity of 24 km/h (with $\lambda = 1$), according to Equations 9 and 13. It may be concluded that sandbags are only effective for relatively low wind velocities. Therefore, sandbags are mostly useful during short periods of time (e.g. during construction) when it is hoped that high velocity winds will not occur.

3 ANALYSIS OF GEOMEMBRANE UPLIFT

3.1 Overview

In Section 2, the conditions under which a geomembrane is uplifted have been reviewed. In Section 3, the mechanism of geomembrane uplift is analyzed and quantified. In particular, the magnitude of geomembrane uplift is determined, and the tension and strain in the geomembrane are calculated.

Parameters and assumptions are presented in Section 3.2. Then, Sections 3.3 and 3.4 are devoted to the development of the general method, which is applicable to all cases of geomembrane tensile behavior. Finally, Section 3.5 is devoted to the case where the geomembrane tension-strain curve is linear and Section 3.6 to the influence of geomembrane temperature on uplift by wind.

3.2 Parameters and Assumptions

The parameters that govern geomembrane uplift are the configuration of the geomembrane, the mechanical behavior of the geomembrane, and the suction exerted by the wind. These parameters are discussed below, along with the related assumptions.

3.2.1 Geomembrane Configuration

A length L of geomembrane is assumed to be subjected to wind suction and the geomembrane movements are assumed to be restrained at both ends of the length L . For example, the geomembrane movements are restrained as follows:

- At the crest of a slope, the geomembrane is typically anchored in an anchor trench (Figure 7a), under a pavement (Figure 7b), or under a structure (Figure 7e).
- At the toe of a slope, the geomembrane may be anchored in an anchor trench (Figure 7a) or its movements are restrained by a layer of soil (Figure 7b).

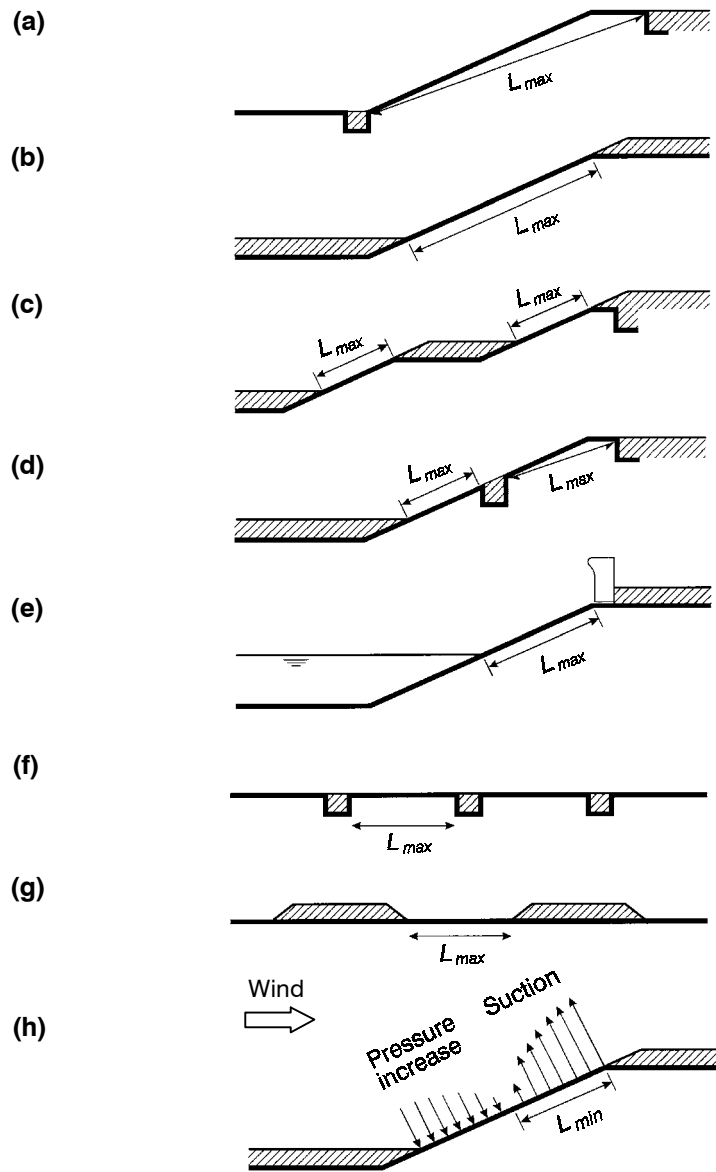


Figure 7. Typical configurations of a geomembrane exposed to wind: (a) geomembrane anchored in an anchor trench; (b) geomembrane anchored under a pavement or a layer of soil; (c) geomembrane restrained by a soil layer on a bench; (d) geomembrane restrained by an intermediate anchor trench; (e) geomembrane anchored under a structure at the top and restrained by liquid or solids at the bottom; (f) at bottom of reservoir, geomembrane anchored in anchor trenches; (g) at bottom of reservoir, geomembrane anchored by strips of soil or pavement; (h) slope partly exposed to pressure increase caused by wind.

(Note: Figure 7h is consistent with the windward slope of Figure 4.)

- At one or several intermediate levels, along a slope, the movements of a geomembrane can be restrained by a soil layer covering the geomembrane on a bench (Figure 7c) or by an intermediate anchor trench (Figure 7d).
- At any level, the movements of the geomembrane can be restrained by the impounded liquid (Figure 7e) or the stored solid material.
- At the bottom of a reservoir, the geomembrane may be anchored in anchor trenches (Figure 7f) or by strips of soil or pavement (Figure 7g).

The anchor trenches and soil layers discussed above are assumed to be adequately sized for the considered winds. Therefore, it is assumed that the wind will not pull the geomembrane out of the anchor trench or from under a soil layer. However, the sizing of anchor trenches and soil layers restricting the movement of geomembranes is beyond the scope of this paper.

In Figures 7a to 7g, a length L_{max} is shown. This is the length of exposed geomembrane between two locations where its movements are restrained. The length, L , of geomembrane subjected to suction due to wind is equal to, or less than, L_{max} . It is less than L_{max} if there are areas where the atmospheric pressure increases as a result of wind, as shown in Figure 7h. The notation L_{min} is used in Figure 7h because the area where atmospheric pressure has increased may not restrain geomembrane movement as effectively as an anchor trench or a layer of soil. The slope shown in Figure 7h is the same as the slope shown in Figure 7b. Using data provided in Figure 4, the design engineer has to select a length L between L_{min} and L_{max} , for the calculations presented in the subsequent sections.

Regardless of its location (on slopes or at the bottom), if the geomembrane is entirely covered with a layer of soil or other heavy material, it should not be uplifted if the condition expressed by Equation 29 is met. Therefore, it is assumed in Section 3 that the geomembrane is not covered. Also, it is assumed that over the length L , where the geomembrane is subjected to wind-generated suction, the geomembrane is not glued to a rigid support or loaded with sandbags. Similarly, it is assumed that there are no suction vents through the geomembrane, or any other mechanism that stabilizes the geomembrane by decreasing the air pressure under the geomembrane when the wind blows. It is also assumed that the medium under the geomembrane is permeable enough that the uplifting of the geomembrane will not be restricted by a decrease in air pressure beneath the geomembrane due to the sudden increase in volume beneath the geomembrane when uplifting begins. In other words, it is assumed that the geomembrane is free to move away from the supporting medium over the length L .

Another simplifying assumption is that the magnitude of the suction does not change in response to changes in geomembrane shape after initial uplift. (It is possible that the initial ballooning of a geomembrane may result in a cylindrical-shaped geometry that will generate a suction larger than that assumed to create initial uplift.) Therefore, the analyses presented in Sections 3.3 to 3.6 are not applicable to geomembranes that have experienced initial uplift leading to a change in aerodynamic flow.

Finally, it is assumed that the geomembrane is sealed around its periphery and, as a result, the wind cannot uplift the geomembrane by reaching beneath it. Therefore, the analyses presented in Sections 3.3 to 3.6 are not applicable to a situation that exists during geomembrane installation where a panel is not seamed at its edge, nor are the analyses applicable to geomembranes that are torn open.

3.2.2 Mechanical Behavior of the Geomembrane

The problem is assumed to be two-dimensional. Therefore, the geomembrane is assumed to be characterized by its tension-strain curve measured in a tensile test that simulates plane-strain conditions. A wide-width tensile test provides a satisfactory approximation of this case. If only results of a uniaxial tensile test are available, the tensile characteristics under plane-strain conditions can be derived from the tensile characteristics under uniaxial conditions as indicated by Soderman and Giroud (1995).

Essential characteristics of geomembranes for use in design are the allowable tension, T_{all} , and strain, ϵ_{all} . Typical tension-strain curves are shown in Figure 8:

- If the geomembrane tension-strain curve has a peak (Curve 1), the allowable tension and strain correspond to the values of T and ϵ at the peak (as shown in Figure 8) or before the peak if a margin of safety is required.
- If the geomembrane tension-strain curve has a plateau (Curve 2), the allowable tension and strain correspond to the values of T and ϵ at the beginning of the plateau (as shown in Figure 8) or before if a margin of safety is required.
- If the geomembrane tension-strain curve has neither peak nor plateau (Curve 3), the allowable tension and strain correspond to the values of T and ϵ at the end of the curve, i.e. at break (as shown in Figure 8), or before if a margin of safety is required.

In all three cases, values of T_{all} and ϵ_{all} that are less than the values given above can be selected for any appropriate reasons (i.e. to meet regulatory requirements, to limit deformations, etc.).

In some cases, the geomembrane tension-strain curve, or a portion of it, is assumed to be linear. Then, the following relationship exists:

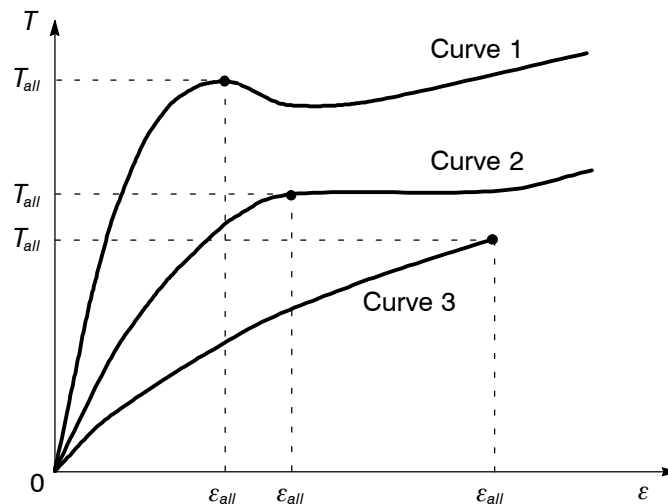


Figure 8. Typical tension-strain curves of geomembranes.

$$T = J \varepsilon \quad (34)$$

where: T = geomembrane tension; J = geomembrane tensile stiffness; and ε = geomembrane strain. The case of geomembranes with a linear tension-strain curve will be further discussed in Section 3.5.

It is important to note that geomembranes that are not reinforced with a fabric, for example PVC and PE geomembranes, have tensile characteristics that are highly dependent on temperature. Extensive data on the influence of temperature on the tensile characteristics of HDPE geomembranes are provided by Giroud (1994). The influence of temperature will be further discussed in Section 3.6.

3.2.3 Suction Due to Wind

In the subsequent analysis, the suction applied by the wind is assumed to be uniform over the entire length L . In reality, the suction due to the wind is not uniformly distributed as shown in Figure 4. Therefore, the design engineer using the method presented in this paper must exercise judgment in selecting the value of the length L and the value of the ratio λ defined by Equation 13.

In accordance with the discussions presented in Sections 2.3 and 2.4, the suction that effectively uplifts the geomembrane is:

$$S_e = S - \mu_{GM} g \quad (35)$$

where S_e is the "effective suction".

Combining Equations 2, 13 and 35 gives:

$$S_e = \lambda \rho V^2 / 2 - \mu_{GM} g \quad (36)$$

Combining Equations 3 and 36 gives:

$$S_e = \lambda \rho_o (V^2 / 2) e^{-\rho_o g z / p_o} - \mu_{GM} g \quad (37)$$

Using the values of ρ_o and p_o given in Section 2.1 and $g = 9.81 \text{ m/s}^2$, Equation 37 gives:

- At sea level:

$$S_e = 0.6465 \lambda V^2 - 9.81 \mu_{GM} \quad (38)$$

with S_e (Pa), V (m/s), μ_{GM} (kg/m²)

$$S_e = 0.050 \lambda V^2 - 9.81 \mu_{GM} \quad (39)$$

with S_e (Pa), V (km/h), μ_{GM} (kg/m²)

- At altitude z above sea level:

$$S_e = 0.6465\lambda V^2 e^{-(1.252 \times 10^{-4})z} - 9.81\mu_{GM} \quad (40)$$

with $S_e(\text{Pa})$, $V(\text{m/s})$, $z(\text{m})$, $\mu_{GM}(\text{kg/m}^2)$

$$S_e = 0.050\lambda V^2 e^{-(1.252 \times 10^{-4})z} - 9.81\mu_{GM} \quad (41)$$

with $S_e(\text{Pa})$, $V(\text{km/h})$, $z(\text{m})$, $\mu_{GM}(\text{kg/m}^2)$

3.3 Determination of Geomembrane Tension and Strain

According to Equation 36, the effective suction results from two components: a component due to the wind-generated suction, which is normal to the geomembrane; and a component due to the geomembrane mass per unit area, which is not normal to the geomembrane. The component due to the geomembrane mass per unit area is generally small compared to the component due to the wind-generated suction. Therefore, the effective suction is essentially normal to the geomembrane. Since the effective suction is taken as normal to the geomembrane and has been assumed to be uniformly distributed over the length L of geomembrane, and since the problem is considered to be two-dimensional (see Section 3.2.2), the cross section of the uplifted geomembrane has a circular shape (Figure 9). As a result, the resultant F of the applied effective suction is equal to the effective suction multiplied by the length of chord AB, i.e. L :

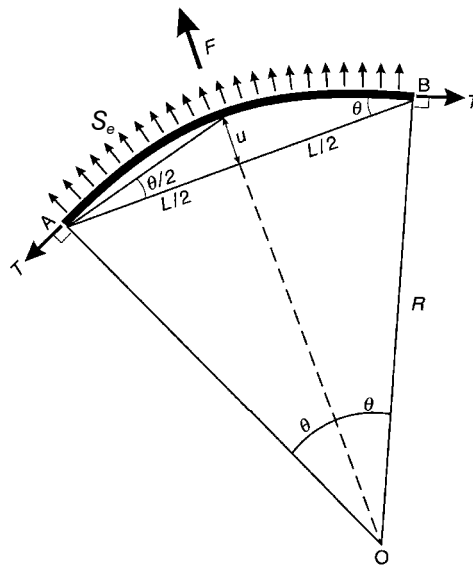


Figure 9. Schematic representation of uplifted geomembrane used for developing equations.

$$F = S_e L \quad (42)$$

The force F is balanced by the geomembrane tensions at the two ends of arc AB. Projecting on the perpendicular to chord AB gives:

$$F = 2T \sin \theta \quad (43)$$

Combining Equations 42 and 43 gives:

$$\frac{T}{S_e L} = \frac{1}{2 \sin \theta} \quad (44)$$

Since the effective suction S_e is uniformly distributed, so is the geomembrane strain, ϵ . Therefore, ϵ can be calculated as follows:

$$1 + \epsilon = \frac{\text{arc AB}}{L} = \frac{2R\theta}{2R \sin \theta} \quad (45)$$

hence:

$$\epsilon = \frac{\theta}{\sin \theta} - 1 \quad (46)$$

Eliminating θ between Equations 44 and 46 gives the following relationship between the strain, ϵ , and the normalized tension, $T/(S_e L)$, in the geomembrane:

$$\epsilon = \frac{2T}{S_e L} \sin^{-1} \left[\frac{S_e L}{2T} \right] - 1 \quad (47)$$

This relationship is represented by a curve shown in Figure 10. (It should be noted that it is not possible to express $T/(S_e L)$ analytically as a function of ϵ .) Numerical values of $T/(S_e L)$ as a function of ϵ are given in Table 2.

The relationship expressed by Equation 47 and represented in Figure 10 is the relationship between the geomembrane tension, T , and strain, ϵ , when the geomembrane is uplifted by an effective suction S_e , over a length L . This is the fundamental relationship of the geomembrane uplift problem and it is referred to as the "uplift tension-strain relationship".

To determine if the considered geomembrane is acceptable regarding wind uplift resistance, its tension-strain curve must be compared to the uplift tension-strain relationship expressed by Equation 47, and represented by the curve in Figure 10. This can be done by plotting on the same graph the curve of the uplift tension-strain relationship and the normalized tension-strain curve of the geomembrane derived from the geomembrane tension-strain curve by dividing the tension by $S_e L$ (Figure 11). The intersection between the two curves gives the normalized tension and the strain in the geomembrane when it is uplifted by the considered wind over the considered length, L .

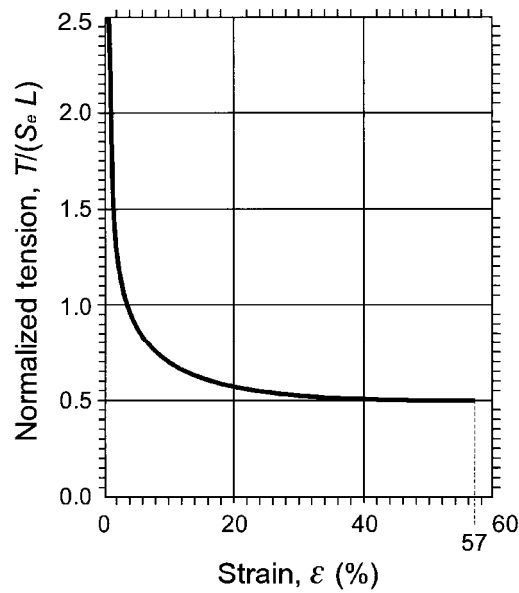


Figure 10. Uplift tension-strain relationship.
 (Note: This curve was established using Equation 47. Numerical values are given in Table 2.)

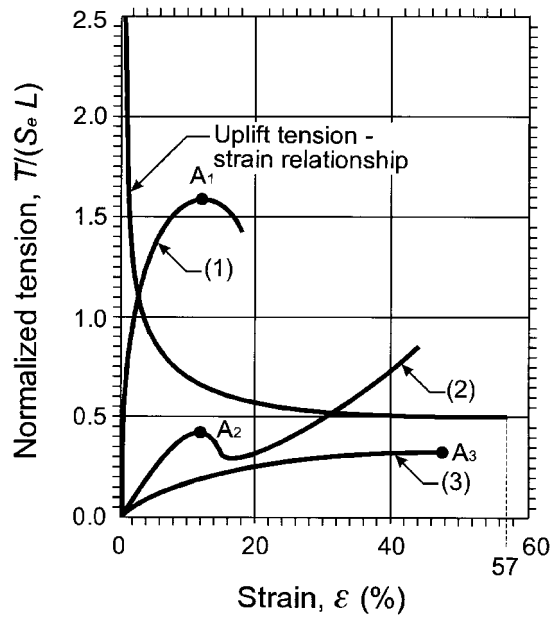


Figure 11. Uplift tension-strain relationship curve (from Figure 10) and normalized tension-strain curves of three different geomembranes plotted on the same graph.
 (Note: Curve (1) has been derived from Figure 12 by dividing T by $S_e L = 14.15$ kN/m, the value used in Example 5.)

Table 2. Values of the geomembrane normalized tension $T/(S_e L)$ as a function of the geomembrane strain, ε , the relative uplift, u/L , and the uplift angle, θ .

Relative uplift u/L (-)	Geomembrane strain ε (%)	Normalized tension $T/(S_e L)$ (-)	Uplift angle θ (°)	Relative uplift u/L (-)	Geomembrane strain ε (%)	Normalized tension $T/(S_e L)$ (-)	Uplift angle θ (°)
0.000	0.000	∞	0	0.250	15.91	0.63	53.1
0.010	0.027	12.51	2.3	0.260	17.15	0.61	54.9
0.020	0.107	6.26	4.6	0.270	18.43	0.60	56.7
0.030	0.240	4.18	6.9	0.280	19.75	0.59	58.5
0.040	0.426	3.15	9.1	0.2819	20.00	0.58	58.8
0.050	0.665	2.53	11.4	0.2892	21.00	0.58	60.1
0.060	0.957	2.11	13.7	0.290	21.10	0.58	60.2
0.0613	1.000	2.07	14.0	0.2965	22.00	0.57	61.3
0.070	1.30	1.82	15.9	0.300	22.50	0.57	61.9
0.080	1.70	1.60	18.2	0.3035	23.00	0.56	62.5
0.0869	2.00	1.48	19.7	0.310	23.93	0.56	63.6
0.090	2.15	1.43	20.4	0.3105	24.00	0.56	63.7
0.100	2.65	1.30	22.6	0.3174	25.00	0.55	64.8
0.1065	3.00	1.23	24.0	0.320	25.39	0.55	65.2
0.110	3.20	1.19	24.8	0.3241	26.00	0.55	65.9
0.120	3.80	1.10	27.0	0.330	26.89	0.54	66.8
0.1232	4.00	1.08	27.7	0.3307	27.00	0.54	67.0
0.130	4.45	1.03	29.1	0.3373	28.00	0.54	68.0
0.138	5.00	0.97	30.9	0.340	28.43	0.54	68.4
0.140	5.15	0.96	31.3	0.3437	29.00	0.54	69.0
0.150	5.90	0.91	33.4	0.350	30.00	0.53	70.0
0.1513	6.00	0.90	33.7	0.360	31.60	0.53	71.5
0.160	6.69	0.86	35.5	0.370	33.23	0.52	73.0
0.1637	7.00	0.85	36.3	0.380	34.90	0.52	74.5
0.170	7.54	0.82	37.6	0.3806	35.00	0.52	74.6
0.1753	8.00	0.80	38.6	0.390	36.60	0.52	75.9
0.180	8.43	0.78	39.6	0.400	38.32	0.51	77.3
0.1862	9.00	0.76	40.9	0.4096	40.00	0.51	78.6
0.190	9.36	0.75	41.6	0.410	40.08	0.51	78.7
0.1965	10.00	0.73	42.9	0.420	41.86	0.51	80.1
0.200	10.35	0.73	43.6	0.430	43.67	0.51	81.4
0.2064	11.00	0.71	44.9	0.4372	45.00	0.50	82.3
0.210	11.37	0.70	45.6	0.440	45.51	0.50	82.7
0.2159	12.00	0.69	46.7	0.450	47.38	0.50	84.0
0.220	12.44	0.68	47.5	0.460	49.27	0.50	85.2
0.2250	13.00	0.67	48.5	0.4638	50.00	0.50	85.7
0.230	13.56	0.66	49.4	0.470	51.18	0.50	86.5
0.2339	14.00	0.65	50.1	0.480	53.13	0.50	87.7
0.240	14.71	0.64	51.3	0.490	55.09	0.50	88.8
0.2424	15.00	0.64	51.7	0.500	57.08	0.50	90.0

Note: This table was established using the equations given in Table 3.

On the basis of the above discussion, the considered geomembrane is acceptable regarding wind uplift resistance if its normalized allowable tension is above the curve of the uplift tension-strain relationship shown in Figures 10 and 11. The normalized allowable tension is defined as:

$$T'_{all} = T_{all}/(S_e L) \quad (48)$$

In Figure 11, the geomembrane represented by Curve (1) is acceptable because its allowable tension and strain are represented by A_1 , which is above the uplift tension-strain curve. In contrast, the geomembranes represented by Curves (2) and (3) are not acceptable (for the considered wind-generated suction, S_e , and exposed length, L) because their allowable tensions and strains are represented by points, A_2 and A_3 , which are below the curve of the uplift tension-strain relationship.

In fact, it is not necessary to draw the entire normalized tension curve of the geomembrane. It is sufficient to plot the allowable tension defined by Equation 48 versus the allowable strain, and to check that it is above the curve of the uplift tension-strain relationship shown in Figures 10 and 11. However, it will be useful to draw the entire curve for the next step of the calculation which consists of determining the deformed shape of the geomembrane, as explained in Section 3.4.

Example 5. A 1.5 mm thick HDPE geomembrane has the tension-strain curve shown in Figure 12, with $T_{all} = 22$ kN/m at $\epsilon_{all} = 12\%$. This geomembrane is installed in a reser-

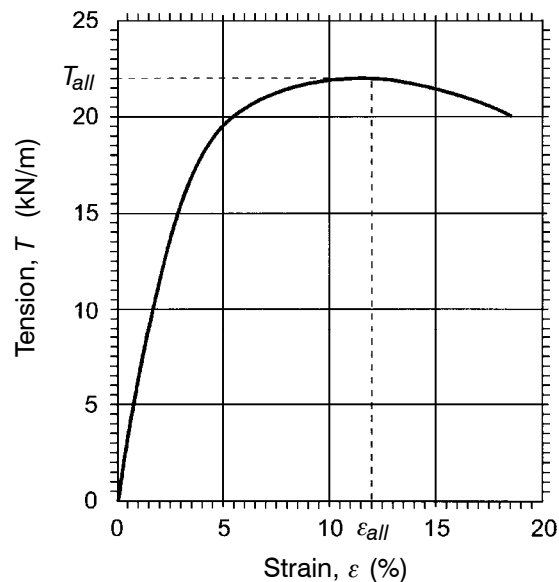


Figure 12. Tension-strain curve of the geomembrane used in Example 5.

(Note: Only the initial portion of the curve is shown, as it is the only portion of the curve relevant to design. The allowable tension and strain are assumed to correspond to the yield peak.)

voir located 300 m above sea level, in an area where, during a certain season, winds with velocities up to 150 km/h can be expected. The bottom of the reservoir is covered with 0.3 m of soil, but the geomembrane is exposed on the 1V:3H side slopes, which are 6 m high. Assuming the geomembrane is properly anchored at the crest of the slope, is this geomembrane acceptable regarding wind uplift resistance if the wind blows at the maximum expected speed?

First, it is necessary to check that geomembrane movements are restrained at the bottom of the reservoir. According to Figure 5, a value $\lambda = 0.4$ can be used for the suction factor at the bottom of the reservoir. A density $\rho_p = 1700 \text{ kg/m}^3$ can be assumed for the soil layer at the bottom of the reservoir. With $\rho_p = 1700 \text{ kg/m}^3$, $\mu_{GM} = 1.41 \text{ kg/m}^2$ (from Table 1), $\lambda = 0.4$, $V = 150 \text{ km/h}$, and $z = 300 \text{ m}$, the required depth of the soil layer at the bottom of the reservoir can be calculated as follows using Equation 33:

$$D_{req} = \frac{1}{1700} \left(-1.41 + (0.005085)(0.4)(150^2)e^{-(1.252 \times 10^{-4})(300)} \right)$$

hence:

$$D_{req} = \frac{1}{1700} (-1.41 + 44.08) = 0.025 \text{ m} = 25 \text{ mm}$$

The actual value of the depth of the soil layer covering the geomembrane at the bottom of the reservoir, $D = 300 \text{ mm}$, is significantly greater than the required value, $D_{req} = 25 \text{ mm}$. Therefore, if it is assumed that the soil is not removed by the wind or another mechanism, there is no risk of geomembrane uplift by the considered wind at the bottom of the reservoir. However, an additional soil mass is needed at the toe of the slope to control localized geomembrane uplift due to the tension in the geomembrane uplifted by the wind along the slope. This will be further discussed in Section 4.2.

At this point, it can be assumed that the geomembrane movements are restrained both at the toe of the slope, as discussed above, and, at the crest of the slope, by the anchor trench. Therefore, the length of geomembrane subjected to wind-generated suction is the length of the slope, which is:

$$L = 6 / \sin[\tan^{-1}(1/3)] = 19.0 \text{ m}$$

According to Section 2.2 and Figure 5, a value $\lambda = 0.7$ is recommended for the suction factor if the entire slope is considered, which is the case here. Using Equation 41 with $\lambda = 0.7$, $V = 150 \text{ km/h}$, $z = 300 \text{ m}$ and $\mu_{GM} = 1.41 \text{ kg/m}^2$, the effective suction is calculated as follows:

$$S_e = (0.05)(0.7)(150^2)e^{-(1.252 \times 10^{-4})(300)} - (9.81)(1.41)$$

hence:

$$S_e = 758.47 - 13.83 = 744.64 \text{ Pa}$$

hence the value of $S_e L$:

$$S_e L = (744.64)(19.0) = 14,148 \text{ N/m} = 14.15 \text{ kN/m}$$

Then, the normalized geomembrane tension can be calculated as follows using Equation 48:

$$T'_{all} = \frac{T_{all}}{S_e L} = \frac{22}{14.15} = 1.56$$

Table 2 shows that, for $\varepsilon = 12\%$, the uplift tension-strain relationship gives $T/(S_e L) = 0.69$. The value of T'_{all} calculated above is greater than 0.69. Therefore, the considered geomembrane is acceptable and should behave safely when it is uplifted by the considered wind on the considered slope.

This is also shown graphically in Figure 11 where Curve (1) is the normalized geomembrane tension-strain curve derived from the tension-strain curve (shown in Figure 12) of the geomembrane considered in Example 5, using $S_e L = 14.15 \text{ kN/m}$.

END OF EXAMPLE 5

To avoid plotting the normalized tension-strain curve, which may be tedious especially if a number of geomembranes are considered, a family of curves representing the uplift tension-strain relationship can be used (Figure 13). An enlargement of a portion of Figure 13 is provided in Figure 14. The use of Figure 13 or 14 is illustrated in the following design example.

Example 6. The same case as in Example 5 is considered, but is solved using Figure 13 or 14 instead of Table 2 or Figure 11.

Here, instead of plotting the normalized tension-strain curve of the geomembrane (as in Figure 11), the actual tension-strain curve from Figure 12 is plotted directly on Figure 13 or 14, which gives Figure 15. Figure 15 is used to check that the geomembrane allowable tension is greater than $S_e L$ for the allowable strain. It immediately appears that point A of the tension-strain curve which corresponds to the allowable tension (22 kN/m) and the allowable strain (12%) is slightly above the “uplift tension-strain relationship curve” for $S_e L = 30 \text{ kN/m}$ and, therefore, clearly above the curve (not shown) for $S_e L = 14.15 \text{ kN/m}$ (a value which was calculated in Example 5).

END OF EXAMPLE 6

3.4 Determination of Geomembrane Uplift

In Section 3.3, it was shown that the tension and strain in the uplifted geomembrane are obtained at the intersection of the geomembrane normalized tension-strain curve with the curve representing the uplift tension-strain relationship (Figure 11). Knowing

the strain, ϵ , in the geomembrane, it is possible to determine the amount of uplift, u , as shown below.

Simple geometric considerations on Figure 9 lead to the following relationship:

$$\sin \theta = \frac{2}{\frac{2u}{L} + \frac{L}{2u}} \quad (49)$$

Equation 49 can also be written:

$$\theta = \sin^{-1} \left[\frac{2}{\frac{2u}{L} + \frac{L}{2u}} \right] \quad (50)$$

Combining Equations 46, 49 and 50 gives:

$$\epsilon = \frac{1}{2} \left(\frac{2u}{L} + \frac{L}{2u} \right) \sin^{-1} \left[\frac{2}{\frac{2u}{L} + \frac{L}{2u}} \right] - 1 \quad (51)$$

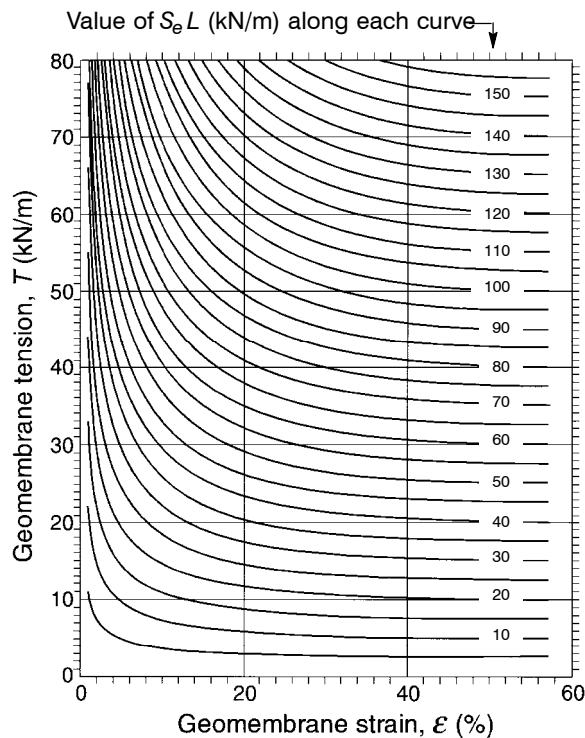


Figure 13. Family of curves representing the uplift tension-strain relationship.

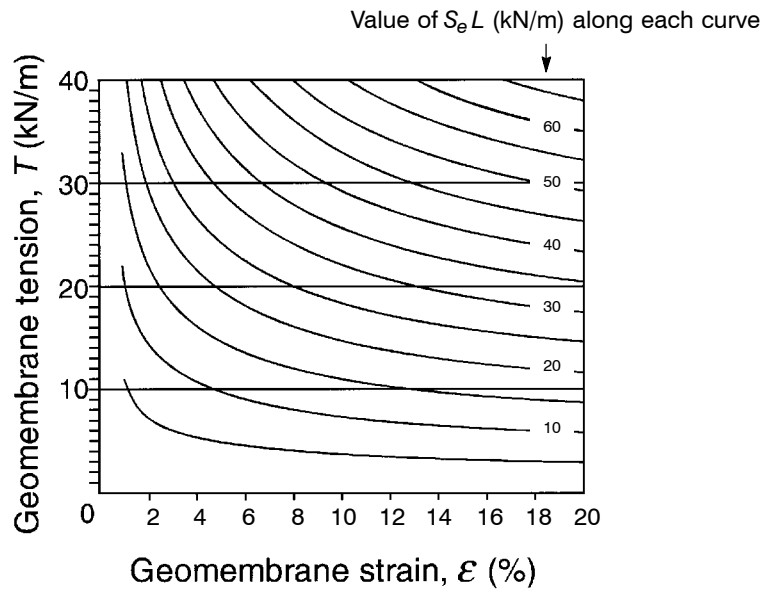


Figure 14. Family of curves representing the uplift tension-strain relationship (enlargement of a portion of the curves in Figure 13).

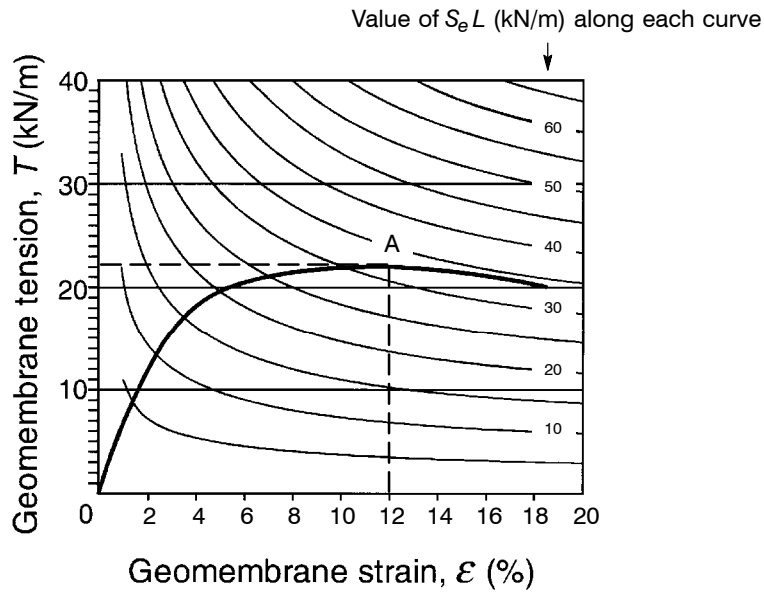


Figure 15. Tension-strain curve of the geomembrane considered in Example 6 (from Figure 12) plotted with the family of curves representing the uplift tension-strain relationship (from Figures 13 and 14).

Combining Equations 44 and 49 gives:

$$\frac{T}{S_e L} = \frac{1}{4} \left(\frac{2u}{L} + \frac{L}{2u} \right) \quad (52)$$

Equation 52 is a quadratic equation in u/L , hence:

$$\frac{u}{L} = \frac{T}{S_e L} - \sqrt{\left(\frac{T}{S_e L} \right)^2 - \frac{1}{4}} \quad (53)$$

Similarly, Equation 49 is a quadratic equation in u/L , hence:

$$\frac{u}{L} = \frac{1 - \cos \theta}{2 \sin \theta} = \frac{1}{2} \tan \left(\frac{\theta}{2} \right) \quad (54)$$

It should be noted that Equation 54 could have been obtained from simple geometric considerations in Figure 9. Equation 54 can be rewritten as follows:

$$\theta = 2 \tan^{-1} \left(\frac{2u}{L} \right) \quad (55)$$

Finally, Equation 44 can be written:

$$\theta = \sin^{-1} \left(\frac{S_e L}{2T} \right) \quad (56)$$

It is useful to calculate the angle θ , because it gives the orientation of the geomembrane tension at both extremities of the geomembrane (Figure 9), which is needed to design the anchor trenches or any other anchor systems.

The geometry of the uplifted geomembrane can be characterized by three parameters: the geomembrane strain, ε ; the geomembrane uplift, u ; and the angle, θ , between the edge of the geomembrane and the supporting soil (see Figure 9). There are nine useful relationships between these parameters, or between these parameters and the normalized tension, $T/(S_e L)$. These relationships are summarized in Table 3 and represented in Figures 10, 16, 17, 18, 19 and 20. Also, the numerical values of these relationships are given in Table 2. Finally, all the relationships are presented together in Figure 21, which is useful to understand the consistency between all the relationships discussed above.

A key step in solving a geomembrane uplift problem, is the determination of the strain in the uplifted geomembrane. As indicated at the beginning of Section 3.4, the strain, ε , is obtained at the intersection of the geomembrane normalized stress-strain curve and the curve that represents the uplift tension-strain relationship. As seen in Figure 11, the value thus obtained for ε is not very precise. For more precision, one may proceed by trial and error using Equation 47 or Table 2, as shown in Example 7.

Table 3. Summary of important relationships.

Parameters	Relationship	Equation no.	Figure no.
$T/(S_e L)$ and u/L	$\frac{T}{S_e L} = \frac{1}{4} \left(\frac{2u}{L} + \frac{L}{2u} \right)$	52	16
$T/(S_e L)$ and θ	$\frac{T}{S_e L} = \frac{1}{2 \sin \theta}$	44	17
ϵ and $T/(S_e L)$	$\epsilon = \frac{2T}{S_e L} \sin^{-1} \left(\frac{S_e L}{2T} \right) - 1$	47	10
ϵ and u/L	$\epsilon = \frac{1}{2} \left(\frac{2u}{L} + \frac{L}{2u} \right) \sin^{-1} \left[\frac{2}{\frac{2u}{L} + \frac{L}{2u}} \right] - 1$	51	18
ϵ and θ	$\epsilon = \frac{\theta}{\sin \theta} - 1$	46	19
θ and $T/(S_e L)$	$\theta = \sin^{-1} \left(\frac{S_e L}{2T} \right)$	56	17
θ and u/L	$\theta = \sin^{-1} \left[\frac{2}{\frac{2u}{L} + \frac{L}{2u}} \right] = 2 \tan^{-1} \left[\frac{2u}{L} \right]$	50 and 55	20
u/L and $T/(S_e L)$	$\frac{u}{L} = \frac{T}{S_e L} - \sqrt{\left(\frac{T}{S_e L} \right)^2 - \frac{1}{4}}$	53	16
u/L and θ	$\frac{u}{L} = \frac{1 - \cos \theta}{2 \sin \theta} = \frac{1}{2} \tan \left(\frac{\theta}{2} \right)$	54	20

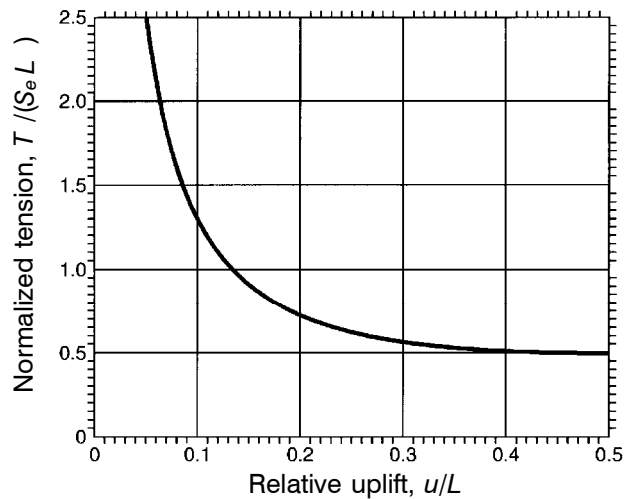


Figure 16. Relationship between the normalized tension in the geomembrane and the relative uplift of the geomembrane.

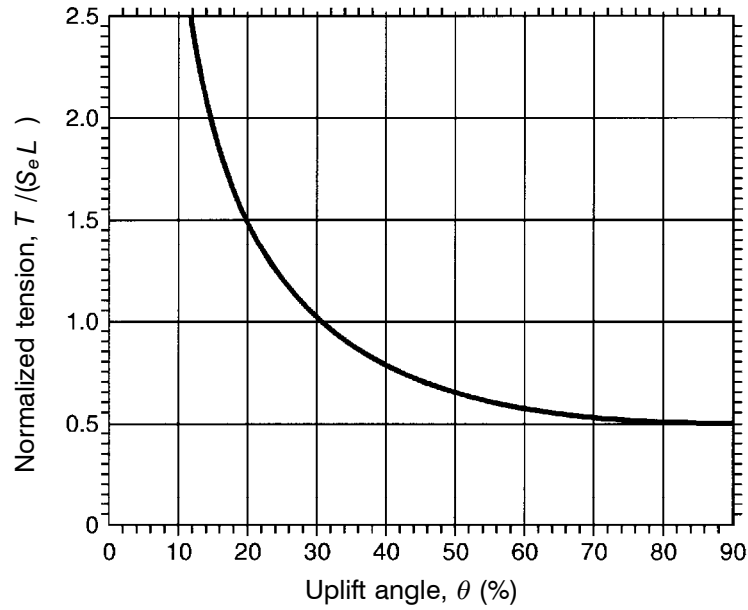


Figure 17. Relationship between the normalized tension in the geomembrane and the uplift angle θ .

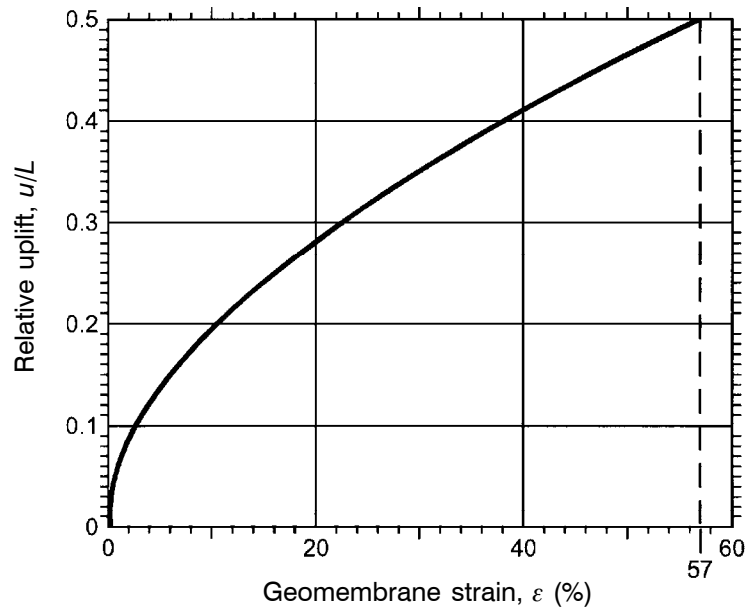


Figure 18. Relationship between the relative uplift and the geomembrane strain.

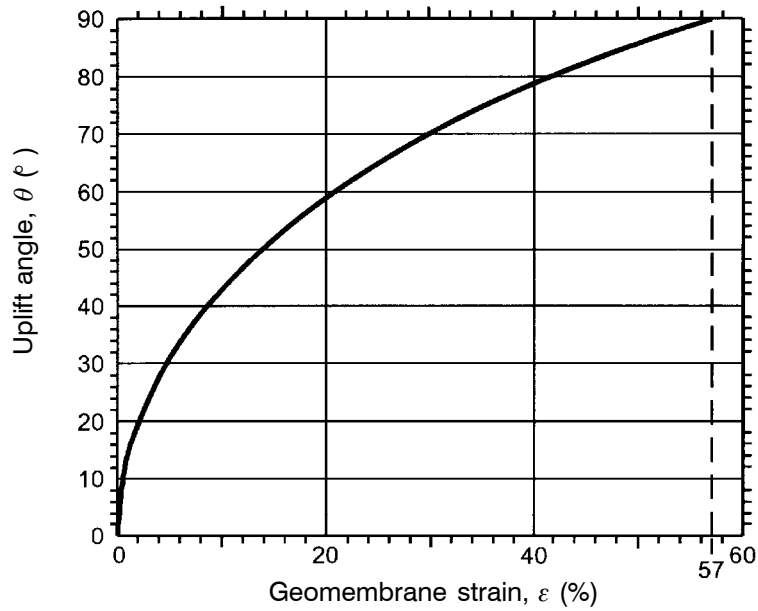


Figure 19. Relationship between the uplift angle and the geomembrane strain.

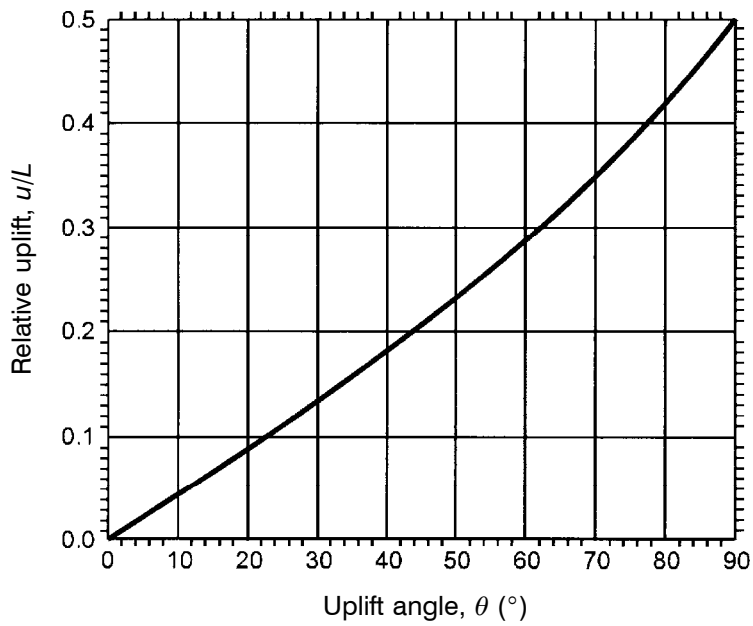


Figure 20. Relationship between the relative uplift and the uplift angle.

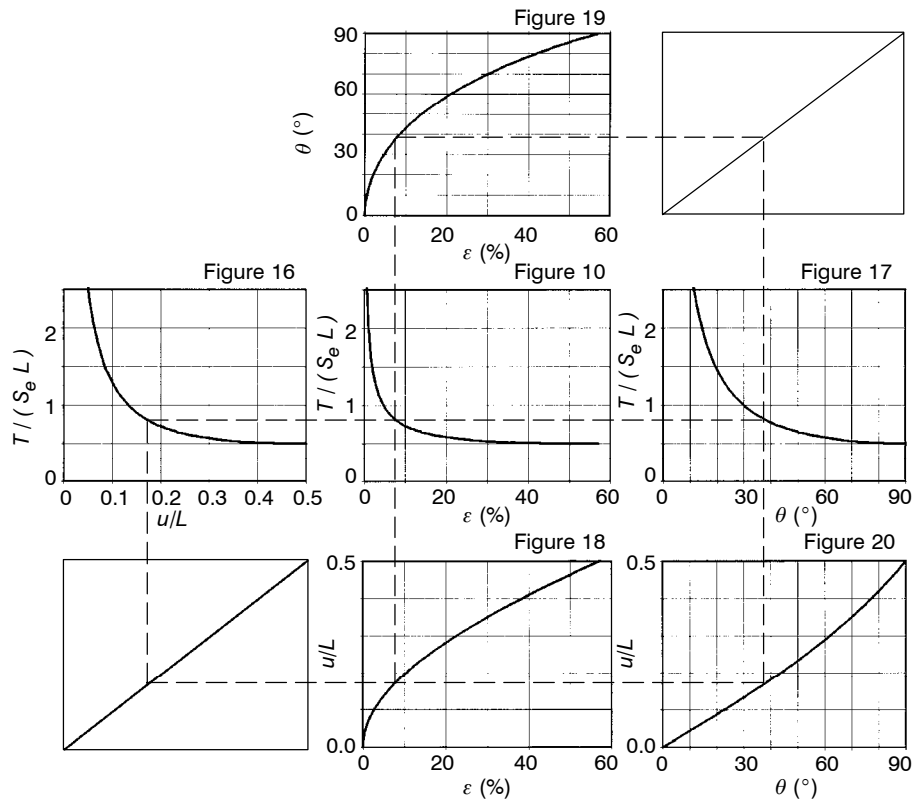


Figure 21. Relationship between Figures 10 and 16 to 20.

Example 7. The same case as in Example 5 is considered. What is the geomembrane strain, ϵ , the geomembrane uplift, u , and the angle, θ , between the extremities of the geomembrane and the slope?

A precise determination of $T/(S_e L)$ and ϵ of the uplifted geomembrane will be done by trial and error using Equation 47. Figure 11 is used to select a starting value of T for the trial and error process. In Figure 11, the value of $T/(S_e L)$ at the intersection of Curve (1) and the curve of the uplift tension-strain relationship appears to be on the order of 1. Since $S_e L = 14.15$ kN/m according to Example 5, a value of $T/(S_e L)$ on the order of 1 leads to a first trial with $T = 14$ kN/m. Equation 47 gives:

$$\epsilon = \frac{(2)(14)}{14.15} \sin^{-1} \frac{14.15}{(2)(14)} - 1 = 0.048 = 4.8\%$$

The calculated value of 4.8% is too large because, for $T = 14$ kN/m, the tension-strain curve of the geomembrane shown in Figure 12 gives $\epsilon = 2.6\%$. A larger value of T is tried: $T = 17$ kN/m. Equation 47 gives:

$$\epsilon = \frac{(2)(17)}{14.15} \sin^{-1} \frac{14.15}{(2)(17)} - 1 = 0.031 = 3.1\%$$

The calculated value of 3.1% is too small because, for $T = 17$ kN/m, the geomembrane tension-strain curve (Figure 12) gives $\epsilon = 3.7\%$. A slightly smaller value of T is tried: $T = 16.4$ kN/m. Equation 47 gives:

$$\epsilon = \frac{(2)(16.4)}{14.15} \sin^{-1} \frac{14.15}{(2)(16.4)} - 1 = 0.034 = 3.4\%$$

This calculated value of ϵ is equal to the value of ϵ shown on the geomembrane tension-strain curve (Figure 12) for $T = 16.4$ kN/m, making the iteration process complete. Therefore, the strain in the uplifted geomembrane is 3.4%, and the tension is 16.4 kN/m.

Instead of using Figure 11 to select a starting value of T for the trial and error process, Table 2 could have been used as follows:

- For $\epsilon = 3.2\%$, $T = 15.8$ kN/m according to Figure 12, hence $T/(S_e L) = 15.8/14.15 = 1.12$, which is less than 1.19 (value given in Table 2 for $\epsilon = 3.2\%$).
- For $\epsilon = 3.8\%$, $T = 17.2$ kN/m according to Figure 12, hence $T/(S_e L) = 17.2/14.15 = 1.22$, which is greater than 1.10 (value given in Table 2 for $\epsilon = 3.8\%$).

Therefore, Table 2 shows that $T/(S_e L)$ is between 1.10 and 1.19, hence a starting value $T = (1.15)(14.15) = 16.3$ kN/m. This value is close to the actual value of 16.4 kN/m. Consequently, iterations using Equation 47 with this starting value would be rapid.

Then, the relative deflection, u/L , can be obtained from $\epsilon = 3.4\%$ using Figure 18, or from $T/(S_e L) = 16.4/(14.15) = 1.16$, using Figure 16, or from Table 2. A value of $u/L \approx 0.115$ is obtained. Alternatively, u/L can be calculated using Equation 53 as follows:

$$\frac{u}{L} = 1.16 - \sqrt{(1.16)^2 - 0.25} = 0.1133$$

hence:

$$u = (0.1133)(19) = 2.15 \text{ m}$$

Finally, the angle θ can be either obtained from Figures 17, 19 or 20, or calculated using Equation 56 as follows:

$$\theta = \sin^{-1} \left[\frac{1}{(2)(1.16)} \right] = 25.5^\circ$$

Alternatively, the angle θ can be calculated using Equation 55 as follows:

$$\theta = 2 \tan^{-1} [(2)(0.1133)] = 25.5^\circ$$

END OF EXAMPLE 7

3.5 Case of a Geomembrane with a Linear Tension-Strain Curve

The method presented in Sections 3.3 and 3.4 is general and no assumption is made regarding the tensile behavior of the geomembrane. As seen in Figures 11 and 12, an HDPE geomembrane is far from having a linear tension-strain curve. However, some reinforced geomembranes have a tension-strain curve which can be considered linear. In this case, the general method presented in Sections 3.3 and 3.4 can be simplified as follows.

Combining Equations 34 and 47 gives:

$$\frac{S_e L}{2J\epsilon} = \sin \left[\frac{S_e L}{2J} \left(1 + \frac{1}{\epsilon} \right) \right] \quad (57)$$

where J is the tensile stiffness of the geomembrane.

In any given case, S_e , L and J are known. Therefore, Equation 57 gives the strain ϵ in the geomembrane. Then the tension, T , can be derived from the strain, ϵ , using Equation 34. The other parameters that characterize the uplift of the geomembrane, u/L and θ , can then be derived from T using Equations 53 and 56, respectively.

Equation 57 can only be solved numerically. The numerical solution is given in Table 4 as a function of the normalized tensile stiffness, $J/(S_e L)$. The use of Equation 57 is illustrated by the following example.

Example 8. The same case as in Example 5 is considered, except that the geomembrane is a reinforced geomembrane with a linear tension-strain curve, a tensile stiffness of 310 kN/m and a strain at break of 23%. In order to have a factor of safety of 2, the allowable strain is 11.5%. What values can be predicted for the strain and tension in the geomembrane when it is uplifted by the considered wind?

To use Table 4, the normalized tensile stiffness must be calculated as follows, using $S_e L = 14.15$ kN/m calculated for Example 5:

$$\frac{J}{S_e L} = \frac{310}{14.15} = 21.9$$

Table 4 gives $\epsilon = 4.6\%$, which is significantly less than the allowable strain of 11.5%. Therefore, the geomembrane should not break when it is uplifted by the wind.

The tension, T , of the uplifted geomembrane can then be calculated using Equation 34:

$$T = (310)(0.046) = 14.3 \text{ kN/m}$$

Then, the uplift can be calculated using Equation 53 as follows:

$$\frac{u}{L} = \frac{14.3}{14.15} - \sqrt{\left(\frac{14.3}{14.15}\right)^2 - \frac{1}{4}} = 0.132$$

hence: $u = (0.132)(19) = 2.5 \text{ m}$

Table 4. Relationship between the strain of the geomembrane uplifted by the wind and the normalized tensile stiffness of the geomembrane for the case where the geomembrane has a linear tension-strain curve (Equation 57).

ε (%)	$\frac{J}{S_e L}$						
0	∞	3.6	31.347	7.2	11.607	10.8	6.607
0.1	6463.688	3.7	30.124	7.3	11.384	10.9	6.525
0.2	2288.342	3.8	28.981	7.4	11.168	11.0	6.443
0.3	1247.294	3.9	27.910	7.5	10.959	11.1	6.365
0.4	811.232	4.0	26.905	7.6	10.757	11.2	6.291
0.5	581.251	4.1	25.960	7.7	10.561	11.3	6.212
0.6	442.767	4.2	25.071	7.8	10.372	11.4	6.138
0.7	351.834	4.3	24.233	7.9	10.189	11.5	6.065
0.8	288.358	4.4	23.442	8.0	10.010	11.6	5.994
0.9	241.983	4.5	22.694	8.1	9.839	11.7	5.925
1.0	206.885	4.6	21.987	8.2	9.671	11.8	5.857
1.1	179.565	4.7	21.316	8.3	9.508	11.9	5.790
1.2	157.804	4.8	20.680	8.4	9.351	12.0	5.724
1.3	140.137	4.9	20.076	8.5	9.198	12.1	5.660
1.4	125.562	5.0	19.502	8.6	9.049	12.2	5.598
1.5	113.368	5.1	18.956	8.7	8.905	12.3	5.537
1.6	103.044	5.2	18.435	8.8	8.765	12.4	5.477
1.7	94.212	5.3	17.939	8.9	8.628	12.5	5.418
1.8	86.586	5.4	17.465	9.0	8.495	12.6	5.359
1.9	79.947	5.5	17.013	9.1	8.365	12.7	5.302
2.0	74.125	5.6	16.580	9.2	8.240	12.8	5.247
2.1	68.985	5.7	16.167	9.3	8.118	12.9	5.192
2.2	64.421	5.8	15.771	9.4	7.998	13.0	5.138
2.3	60.345	5.9	15.392	9.5	7.882	13.1	5.086
2.4	56.688	6.0	15.027	9.6	7.769	13.2	5.035
2.5	53.391	6.1	14.678	9.7	7.658	13.3	4.984
2.6	50.407	6.2	14.342	9.8	7.551	13.4	4.934
2.7	47.696	6.3	14.020	9.9	7.446	13.5	4.885
2.8	45.223	6.4	13.710	10.0	7.344	13.6	4.837
2.9	42.960	6.5	13.412	10.1	7.243	13.7	4.790
3.0	40.885	6.6	13.126	10.2	7.146	13.8	4.743
3.1	38.973	6.7	12.849	10.3	7.051	13.9	4.698
3.2	37.209	6.8	12.582	10.4	6.958	14.0	4.653
3.3	35.577	6.9	12.325	10.5	6.867	14.1	4.609
3.4	34.064	7.0	12.078	10.6	6.779	14.2	4.566
3.5	32.657	7.1	11.838	10.7	6.692	14.3	4.524

Table 4. (Continued)

ε (%)	$\frac{J}{S_e L}$						
14.4	4.482	18.0	3.345	21.6	2.651	25.2	2.189
14.5	4.441	18.1	3.321	21.7	2.635	25.3	2.178
14.6	4.400	18.2	3.297	21.8	2.620	25.4	2.168
14.7	4.361	18.3	3.274	21.9	2.605	25.5	2.157
14.8	4.322	18.4	3.251	22.0	2.590	25.6	2.147
14.9	4.283	18.5	3.229	22.1	2.576	25.7	2.137
15.0	4.246	18.6	3.206	22.2	2.561	25.8	2.127
15.1	4.209	18.7	3.184	22.3	2.547	25.9	2.117
15.2	4.172	18.8	3.163	22.4	2.532	26.0	2.107
15.3	4.136	18.9	3.141	22.5	2.518	26.1	2.097
15.4	4.101	19.0	3.120	22.6	2.504	26.2	2.087
15.5	4.066	19.1	3.099	22.7	2.491	26.3	2.077
15.6	4.031	19.2	3.078	22.8	2.477	26.4	2.068
15.7	3.998	19.3	3.058	22.9	2.464	26.5	2.059
15.8	3.964	19.4	3.038	23.0	2.450	26.6	2.049
15.9	3.932	19.5	3.018	23.1	2.437	26.7	2.040
16.0	3.900	19.6	2.998	23.2	2.424	26.8	2.031
16.1	3.868	19.7	2.979	23.3	2.411	26.9	2.021
16.2	3.836	19.8	2.960	23.4	2.399	27.0	2.012
16.3	3.806	19.9	2.941	23.5	2.386	27.1	2.003
16.4	3.776	20.0	2.922	23.6	2.373	27.2	1.994
16.5	3.745	20.1	2.905	23.7	2.361	27.3	1.986
16.6	3.716	20.2	2.885	23.8	2.348	27.4	1.977
16.7	3.687	20.3	2.867	23.9	2.336	27.5	1.968
16.8	3.658	20.4	2.849	24.0	2.324	27.6	1.960
16.9	3.630	20.5	2.832	24.1	2.312	27.7	1.951
17.0	3.602	20.6	2.814	24.2	2.301	27.8	1.943
17.1	3.575	20.7	2.797	24.3	2.289	27.9	1.934
17.2	3.548	20.8	2.780	24.4	2.278	28.0	1.926
17.3	3.521	20.9	2.763	24.5	2.266	28.1	1.918
17.4	3.495	21.0	2.747	24.6	2.255	28.2	1.910
17.5	3.469	21.1	2.730	24.7	2.243	28.3	1.902
17.6	3.444	21.2	2.714	24.8	2.232	28.4	1.894
17.7	3.418	21.3	2.698	24.9	2.221	28.5	1.886
17.8	3.393	21.4	2.682	25.0	2.210	28.6	1.878
17.9	3.369	21.5	2.666	25.1	2.199	28.7	1.870

Table 4. (Continued)

ε (%)	$\frac{J}{S_e L}$						
28.8	1.862	32.4	1.620	36.0	1.435	39.6	1.289
28.9	1.854	32.5	1.615	36.1	1.431	39.7	1.286
29.0	1.847	32.6	1.609	36.2	1.426	39.8	1.282
29.1	1.840	32.7	1.603	36.3	1.422	39.9	1.279
29.2	1.832	32.8	1.598	36.4	1.417	40.0	1.275
29.3	1.824	32.9	1.592	36.5	1.413	40.1	1.271
29.4	1.817	33.0	1.586	36.6	1.408	40.2	1.268
29.5	1.810	33.1	1.581	36.7	1.404	40.3	1.265
29.6	1.802	33.2	1.575	36.8	1.400	40.4	1.261
29.7	1.795	33.3	1.570	36.9	1.395	40.5	1.258
29.8	1.788	33.4	1.564	37.0	1.391	40.6	1.254
29.9	1.781	33.5	1.559	37.1	1.387	40.7	1.251
30.0	1.774	33.6	1.553	37.2	1.383	40.8	1.248
30.1	1.767	33.7	1.548	37.3	1.379	40.9	1.244
30.2	1.760	33.8	1.542	37.4	1.374	41.0	1.241
30.3	1.753	33.9	1.538	37.5	1.370	41.1	1.237
30.4	1.746	34.0	1.532	37.6	1.367	41.2	1.234
30.5	1.739	34.1	1.527	37.7	1.362	41.3	1.231
30.6	1.733	34.2	1.522	37.8	1.359	41.4	1.228
30.7	1.726	34.3	1.517	37.9	1.354	41.5	1.224
30.8	1.719	34.4	1.512	38.0	1.350	41.6	1.221
30.9	1.713	34.5	1.507	38.1	1.346	41.7	1.218
31.0	1.706	34.6	1.502	38.2	1.342	41.8	1.214
31.1	1.700	34.7	1.497	38.3	1.338	41.9	1.211
31.2	1.694	34.8	1.492	38.4	1.334	42.0	1.208
31.3	1.687	34.9	1.487	38.5	1.330	42.1	1.205
31.4	1.681	35.0	1.482	38.6	1.327	42.2	1.202
31.5	1.675	35.1	1.477	38.7	1.323	42.3	1.199
31.6	1.668	35.2	1.472	38.8	1.319	42.4	1.196
31.7	1.662	35.3	1.468	38.9	1.315	42.5	1.193
31.8	1.656	35.4	1.463	39.0	1.311	42.6	1.190
31.9	1.650	35.5	1.458	39.1	1.308	42.7	1.187
32.0	1.644	35.6	1.453	39.2	1.304	42.8	1.184
32.1	1.638	35.7	1.449	39.3	1.301	42.9	1.181
32.2	1.632	35.8	1.444	39.4	1.297	43.0	1.178
32.3	1.626	35.9	1.440	39.5	1.293	43.1	1.175

Table 4. (Continued)

ε (%)	$\frac{J}{S_e L}$						
43.2	1.172	46.8	1.075	50.4	0.995	54.0	0.926
43.3	1.169	46.9	1.073	50.5	0.992	54.1	0.925
43.4	1.166	47.0	1.070	50.6	0.990	54.2	0.923
43.5	1.163	47.1	1.068	50.7	0.989	54.3	0.921
43.6	1.160	47.2	1.065	50.8	0.986	54.4	0.919
43.7	1.157	47.3	1.063	50.9	0.984	54.5	0.918
43.8	1.154	47.4	1.061	51.0	0.982	54.6	0.916
43.9	1.151	47.5	1.058	51.1	0.980	54.7	0.914
44.0	1.149	47.6	1.056	51.2	0.978	54.8	0.913
44.1	1.146	47.7	1.054	51.3	0.976	54.9	0.911
44.2	1.143	47.8	1.051	51.4	0.974	55.0	0.909
44.3	1.140	47.9	1.049	51.5	0.973	55.1	0.908
44.4	1.137	48.0	1.047	51.6	0.971	55.2	0.906
44.5	1.135	48.1	1.044	51.7	0.969	55.3	0.904
44.6	1.132	48.2	1.042	51.8	0.967	55.4	0.903
44.7	1.129	48.3	1.040	51.9	0.965	55.5	0.901
44.8	1.127	48.4	1.038	52.0	0.963	55.6	0.899
44.9	1.124	48.5	1.035	52.1	0.961	55.7	0.898
45.0	1.121	48.6	1.033	52.2	0.959	55.8	0.896
45.1	1.118	48.7	1.031	52.3	0.957	55.9	0.895
45.2	1.116	48.8	1.029	52.4	0.955	56.0	0.893
45.3	1.113	48.9	1.026	52.5	0.953	56.1	0.891
45.4	1.111	49.0	1.024	52.6	0.952	56.2	0.890
45.5	1.108	49.1	1.022	52.7	0.950	56.3	0.888
45.6	1.105	49.2	1.020	52.8	0.948	56.4	0.887
45.7	1.103	49.3	1.018	52.9	0.946	56.5	0.885
45.8	1.100	49.4	1.016	53.0	0.944	56.6	0.883
45.9	1.098	49.5	1.013	53.1	0.942	56.7	0.882
46.0	1.095	49.6	1.011	53.2	0.941	56.8	0.880
46.1	1.093	49.7	1.009	53.3	0.939	56.9	0.879
46.2	1.090	49.8	1.007	53.4	0.937	57.0	0.877
46.3	1.088	49.9	1.005	53.5	0.935	57.08	0.876
46.4	1.085	50.0	1.003	53.6	0.933		
46.5	1.082	50.1	1.001	53.7	0.932		
46.6	1.080	50.2	0.999	53.8	0.930		
46.7	1.078	50.3	0.997	53.9	0.928		

Finally, the angle θ is obtained using Equation 56 as follows:

$$\theta = \sin^{-1} \left[\frac{14.15}{(2)(14.3)} \right] = 29.7^\circ$$

Alternatively, the angle θ can be calculated using Equation 55 as follows:

$$\theta = 2 \tan^{-1} [(2)(0.1324)] = 29.7^\circ$$

END OF EXAMPLE 8

3.6 Influence of Geomembrane Temperature on Uplift by Wind

All geomembranes have a tensile behavior that depends on temperature, especially geomembranes that are not reinforced with a fabric, such as the common types of HDPE and PVC geomembranes. For these geomembranes, the tension-strain curve at high temperature is characterized as follows compared to the tension strain-curve at a lower temperature:

- the tensile stiffness (i.e. the modulus multiplied by thickness) is smaller;
- the maximum tension is smaller;
- the allowable tension (assuming it is defined in the same way in both cases) is smaller;
- the maximum strain is larger; and
- the allowable strain (assuming it is defined in the same way in both cases) is larger.

This is illustrated in Figure 22, which shows the tension-strain curves of a geomembrane at two different temperatures and their intersections with the curve of the uplift tension-strain relationship. It appears in Figure 22 that, for a given wind-generated suction, the geomembrane at high temperature undergoes a smaller tension and a larger strain than at low temperature. It should not be concluded that uplift by wind is safer for a geomembrane at high temperature than at low temperature because the tension is smaller. The criterion that evaluates safety is the ratio between the allowable tension of the considered geomembrane and the calculated tension in the uplifted geomembrane. The greater the ratio, the greater the safety.

As various geomembranes have different tension-strain curves, it is not possible to draw general conclusions: for some geomembranes, the conditions at high temperature may be safer, whereas for other geomembranes, the conditions at low temperature may be safer. In the case of HDPE geomembranes, a conclusion can be drawn because the effect of temperature on tensile behavior is well documented (Giroud 1994). In Figure 23, the curves of the yield tension as a function of the yield strain for a 1 mm thick and a 1.5 mm thick HDPE geomembrane for temperatures ranging between -20°C and 80°C have been plotted on the same graph as the family of curves that represent the "uplift tension-strain relationship". For the sake of this discussion, the yield tension and the yield strain can be considered as the allowable tension and strain of the geomem-

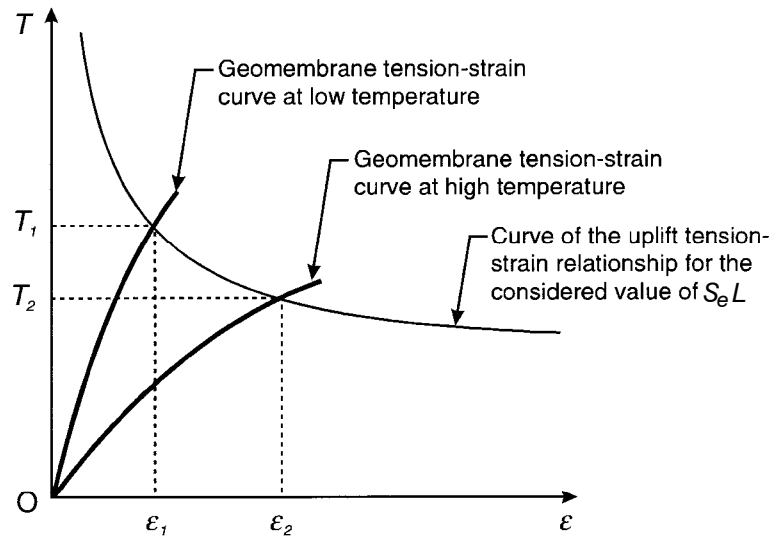


Figure 22. Influence of geomembrane temperature on the tension and strain of the uplifted geomembrane.

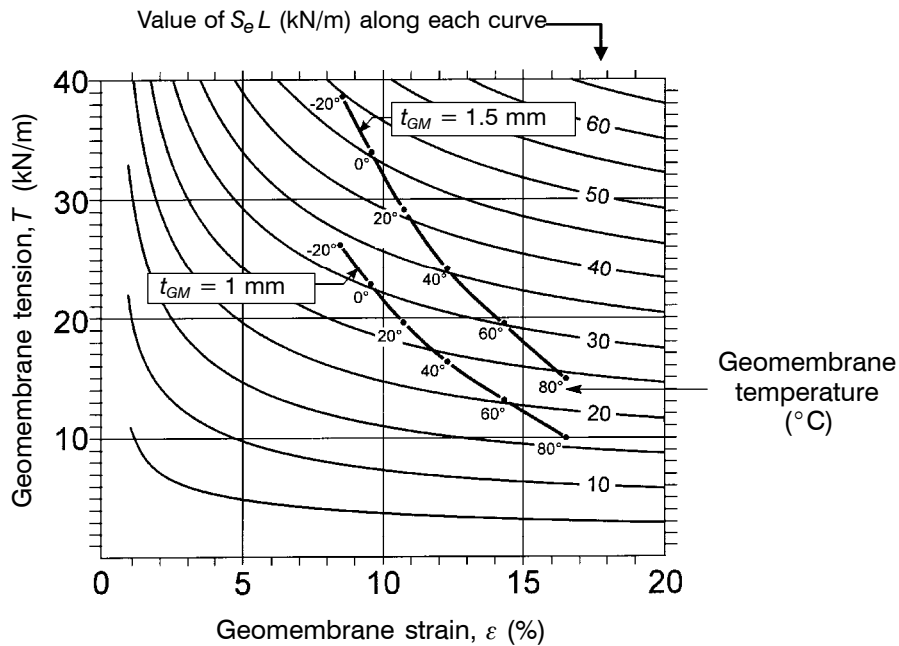


Figure 23. Curves representing a typical relationship between yield tension and yield strain of 1.0 and 1.5 mm thick HDPE geomembranes (from Giroud 1994) plotted on the same graph as the family of curves representing the uplift tension-strain relationship (from Figure 13).

brane. It appears clearly in Figure 23 that HDPE geomembranes better resist wind uplift at low temperatures than at high temperatures. For example, a 1 mm thick HDPE geomembrane would reach yield in a situation characterized by a $S_e L$ value of approximately 30 kN/m at 0°C and 20 kN/m at 60°C. Therefore, when evaluating the uplift resistance of an HDPE geomembrane, the highest possible temperature should be considered to calculate the factor of safety conservatively. However, the lowest possible temperature should also be considered because, in this case, the tension in the uplifted geomembrane has its highest value, which should be used for anchor trench design.

It should also be noted that, in actual design situations, the comparison between geomembrane uplift at high and low temperature is complicated by the fact that wind velocity is often different in the winter and in the summer. This situation is illustrated in Example 9.

Example 9. A geomembrane, with a mass per unit area of 1.8 kg/m², installed in a reservoir located at the sea level is exposed to a wind velocity of 90 km/h in the winter and 140 km/h in the summer. Typical temperatures of the geomembrane when the wind blows are 0°C in the winter and 50°C in the summer. The tension-strain curve of the geomembrane is assumed to be linear with a tensile stiffness of 900 kN/m at 0°C and 400 kN/m at 50°C. What is the geomembrane tension on slopes that are 17 m long?

First, the situation in the winter is considered. Equation 39 gives the effective suction as follows:

$$S_e = (0.05)(0.7)(90^2) - (9.81)(1.8) = 283.5 - 17.7 = 265.8 \text{ Pa}$$

hence:

$$S_e L = (265.8)(17) = 4519 \text{ N/m} = 4.52 \text{ kN/m}$$

Then, the normalized tensile stiffness is obtained as follows:

$$\frac{J}{S_e L} = \frac{900}{4.52} = 199.1$$

For $J/(S_e L) = 199$, Table 4 gives $\varepsilon = 1.0\%$. Then Equation 34 gives:

$$T = (0.010)(900) = 9.0 \text{ kN/m}$$

Then it is useful to calculate θ to have the orientation of the tension T , which is necessary to design the anchor trench. The angle θ is calculated as follows using Equation 56:

$$\theta = \sin^{-1} \left[\frac{4.52}{(2)(9.0)} \right] = 14.5^\circ$$

Second, the situation in the summer is considered. Equation 39 gives the effective suction as follows:

$$S_e = (0.05)(0.7)(140^2) - (9.81)(1.8) = 686.0 - 17.7 = 668.3 \text{ Pa}$$

hence:

$$S_e L = (668.3)(17) = 11,361 \text{ N/m} = 11.36 \text{ kN/m}$$

Then, the normalized tensile stiffness is obtained as follows:

$$\frac{J}{S_e L} = \frac{400}{11.36} = 35.2$$

For $J/(S_e L) = 35$, Table 4 gives $\varepsilon = 3.3\%$. Then Equation 34 gives:

$$T = (0.033)(400) = 13.2 \text{ kN/m}$$

It appears that the tension is greater in the summer than in the winter. This is because the higher wind velocity in the summer has overcome the effect of the higher geomembrane stiffness in the winter. This is illustrated in Figure 24.

The orientation, θ , of the tension is then calculated as follows using Equation 56:

$$\theta = \sin^{-1} \left[\frac{11.4}{(2)(13.2)} \right] = 25.6^\circ$$

————— END OF EXAMPLE 9 —————

In all the calculations and discussions presented in Section 3, it has been implicitly assumed that the geomembrane has no wrinkles and no tension just before wind uplift occurs. In reality, at high temperature, the geomembrane may exhibit wrinkles and, at low temperature, the geomembrane may be under tension as a result of restrained contraction. Both cases can easily be addressed by moving the geomembrane tension-strain curve laterally by an amount ε_T , which is the thermal contraction or expansion of the geomembrane calculated as follows:

$$\varepsilon_T = \alpha(\Gamma - \Gamma_{base}) \quad (58)$$

where: α = coefficient of thermal expansion-contraction of the geomembrane; Γ = temperature of the geomembrane when uplift occurs; and Γ_{base} = temperature of the geomembrane when it rests on the supporting ground without wrinkles and without tension. (This case is referred to as the base case hereinafter.)

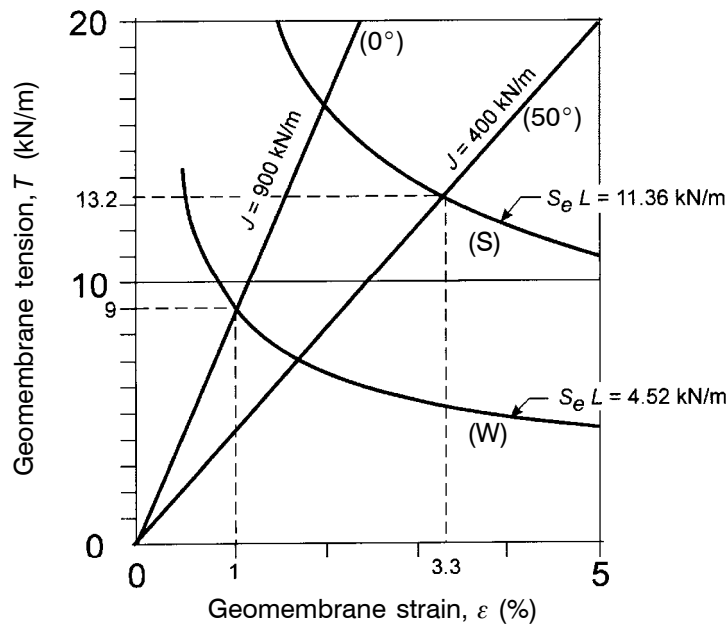


Figure 24. Illustration of Example 9.

(Notes: The curves are as follows: straight lines for the geomembrane tension-strain curve at 0°C (Curve 0°) and at 50°C (Curve 50°); curves representing the uplift tension-strain relationship for a wind velocity of 90 km/h in the winter (Curve W) and for a wind velocity of 140 km/h in the summer (Curve S).)

The foregoing discussion is illustrated in Figure 25 which shows the following:

- If the geomembrane has wrinkles when uplifting begins, its behavior is represented by Curve 1 (i.e. $\epsilon_T > 0$ because $\Gamma > \Gamma_{base}$). The figure shows that, for a given value of $S_e L$, the apparent strain, ϵ_{app1} , in the uplifted geomembrane is greater than the strain, ϵ_{base} , in the uplifted geomembrane for the base case where the geomembrane has no wrinkles or tension when uplifting begins (i.e. $\epsilon_{app1} > \epsilon_{base}$). Since the geometry of the uplifted geomembrane (u, θ) is governed by the apparent strain, a geomembrane is uplifted more (i.e. u and θ are larger) if it has wrinkles at the beginning of uplifting than if it has no wrinkles. The figure also shows that the tension in the uplifted geomembrane, T_1 , is less than it would be in the base case where the geomembrane has no wrinkles or tension when uplifting begins (i.e. $T_1 < T_{base}$). The tension, T_1 corresponds to an actual strain $\epsilon_1 = \epsilon_{app1} - \epsilon_T < \epsilon_{base}$. In summary, if a geomembrane has wrinkles when uplifting begins, it is uplifted more, but with a smaller tension, than if the geomembrane has no wrinkles when uplifting begins.
- If the geomembrane is under tension when uplifting begins, its behavior is represented by Curve 2 (i.e. $\epsilon_T < 0$ because $\Gamma < \Gamma_{base}$). The figure shows that, for a given value of $S_e L$, the apparent strain, ϵ_{app2} , in the uplifted geomembrane is less than the strain, ϵ_{base} , in the uplifted geomembrane for the base case where the geomembrane has no tension or wrinkles when uplifting begins (i.e. $\epsilon_{app2} < \epsilon_{base}$). Since the geometry

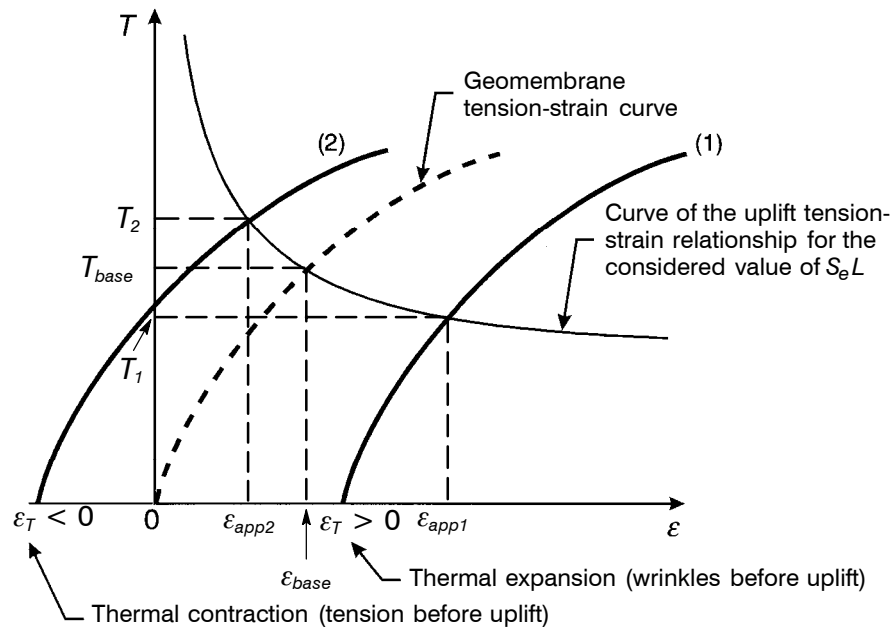


Figure 25. Uplift by the wind of a geomembrane with wrinkles at high temperature (Curve 1) and tension before uplift at low temperature (Curve 2).

(Note: Both Curves 1 and 2 are derived from the geomembrane tension-strain curve by translation parallel to the $O\epsilon$ axis.)

of the uplifted geomembrane (u, θ) is governed by the apparent strain, a geomembrane is uplifted less (i.e. u and θ are less) if it is under tension when uplifting begins than if it is not. The figure also shows that the tension in the uplifted geomembrane, T_2 , is greater than it would be in the base case where the geomembrane has no tension or wrinkles when uplifting begins (i.e. $T_2 > T_{base}$). The tension, T_2 corresponds to an actual strain $\epsilon_2 = \epsilon_{app2} - \epsilon_T = \epsilon_{app2} + |\epsilon_T| > \epsilon_{base}$. In summary, if a geomembrane is under tension when uplifting begins, it is uplifted less, but with a greater tension, than if the geomembrane is not under tension when uplifting begins.

4 PRACTICAL RECOMMENDATIONS

4.1 Recommendations for Preventing Geomembrane Uplift

From the above discussions and design examples, it appears that geomembranes, even those that are heavy, can be significantly uplifted by the wind and can be damaged as explained in Section 1. It is therefore important to try to prevent uplift of geomembranes by wind.

4.1.1 *Protective Cover*

A layer of heavy material, such as soil (assuming it is not removed by the wind), concrete, or equivalent, covering the entire geomembrane, or certain parts most likely to be uplifted, is an effective preventive measure. Equations have been provided in Section 2.4 to calculate the required thickness of such protective covers. Examples have shown that a thickness of a few centimeters is generally sufficient.

4.1.2 *Impounded Liquid*

A rather small depth of liquid, at the bottom of a reservoir, can prevent geomembrane uplift. Equations have been provided in Section 2.4 to calculate the required depth of liquid (typically 100 to 300 mm). A factor of safety is recommended because the wind may displace the liquid and locally decrease the depth of liquid.

4.1.3 *Sandbags*

Sandbags are only effective for winds with a rather small velocity. It has been shown in Section 2.4 that, to ensure uplift prevention in case of high-velocity winds, the number of sandbags would be prohibitive. Also, sandbags can be harmful to the geomembrane for the case of high-velocity winds because they can be displaced when the geomembrane is uplifted and could damage the geomembrane as they move. Sandbags are most effective during construction to prevent the geomembrane from being displaced by low-velocity winds. It is more effective to use a line of adjacent sandbags along the edge of the geomembrane panel just installed than to scatter the sandbags on the installed geomembrane; calculations presented in this paper have shown that scattered sandbags are not very effective, whereas a line of adjacent sandbags at the edge of the installed geomembrane prevents air from flowing under the geomembrane, a major cause of geomembrane uplift.

4.1.4 *Suction Vents*

Suction vents located at the top of slopes are generally believed to be an effective way to prevent or reduce uplift of a geomembrane by the wind. These vents stabilize the geomembrane by sucking air from beneath the geomembrane when the wind blows, thereby decreasing the air pressure beneath the geomembrane. For the suction vents to work, air located beneath the geomembrane must flow toward the vent when the air vent is exposed to wind-generated suction. If the soil beneath the geomembrane has a low permeability, there is little air beneath the geomembrane. This air will flow toward the vent after the geomembrane has been slightly uplifted. If the soil beneath the geomembrane is permeable there is a significant amount of air entrapped beneath the geomembrane, and while this air is being sucked out by the suction vent, the geomembrane is uplifted. Therefore, in all cases the geomembrane may be uplifted for a short period of time before the suction vents are effective. In cases where the soil beneath the geomembrane has a low permeability, short strips of drainage geocomposites, radiating from the suction vent, have been recommended to help drain the air located beneath the geomembrane. However, the effectiveness of this method has not been evaluated.

To the best of the authors' knowledge, no method is available to design suction vents. Ideally, the design of suction vents should address the following: size and configuration of the vent; spacing between vents; and required permeability of the material located beneath the geomembrane. The only point that is well established is that the vents must be at the crest or, at the top of the slope near the crest, in accordance with the data presented in Section 2.2. In a number of projects, suction vents have been placed every 15 m along the periphery of ponds. The reason for selecting 15 m as the spacing is not known. The shape of the suction vents should be such that precipitation water and runoff water are prevented from entering the vent.

4.1.5 *Plastic Tubes and Sandbags Associated with Suction Vents*

Sand-filled plastic tubes or rows of sandbags running from the crest to the toe of slopes are sometimes proposed in conjunction with suction vents. This is a logical combination because sandbags or sand-filled tubes are most effective in case of low-velocity winds and are effective without any delay, whereas suction vents (which are generally considered to be effective at any wind velocity) require some time to be effective, as explained above. It is important to make sure that the tubes or the row of bags do not hamper circulation of air beneath the geomembrane, which is required for the functioning of the suction vents. Therefore such tubes or rows of sandbags should be placed midway between two consecutive suction vents and, if it has been determined that suction vents are necessary, there should not be two parallel tubes or rows of adjacent sandbags without a suction vent in between.

4.1.6 *Vacuum*

Geomembranes used as landfill covers are rarely left exposed. However, such a design may be considered in areas where the use of an exposed geomembrane is aesthetically acceptable and if precautions are taken to ensure that the geomembrane is not damaged by the wind.

The suction exerted by the wind on a landfill may be calculated using Equation 37 with the values of λ summarized in Figure 5, which were initially established for structures associated with reservoirs. However, consistent with recommendations made in Section 2.2, values of λ increased by up to 30% or additional studies, such as wind-tunnel tests of reduced-scale models and numerical simulations, may be warranted in the case of landfills that have an unusual shape.

The use of suction vents to prevent geomembrane uplift by wind is not recommended in the case of a landfill because such vents may promote the infiltration of air into the landfill, which is undesirable because oxygen: inhibits the anaerobic process of waste decomposition; may promote fires in the waste; and may, under certain conditions, create an explosive mixture with methane. Some landfills are equipped with an active gas collection system to collect the methane generated as a result of anaerobic decomposition of the waste. These active gas collection systems comprise blowers that maintain a vacuum in a network of perforated pipes located in the waste. Typically, the magnitude of the vacuum is on the order of 10 kPa at the blower and is less throughout the network of perforated pipes. Active gas collection systems are typically not designed to apply any significant vacuum immediately beneath the landfill cover system, in order

to minimize the risk of air infiltration into the landfill. However, it should be possible to modify an active gas collection system to apply a small vacuum (such as 1 to 2 kPa, according to Figure 3) beneath the geomembrane to prevent geomembrane uplift by the wind. This could be achieved by placing some of the perforated pipes relatively close to the geomembrane cover. These pipes, would mostly be dedicated to the prevention of geomembrane uplift, and would only be activated when the wind starts blowing. The vacuum system should be designed so that the required vacuum (e.g. 2 kPa) can be established beneath the geomembrane before the wind velocity reaches its maximum value. It is important that the blowers for the pipe network dedicated to geomembrane uplift prevention be supplied with electricity regardless of wind velocity, even though high-velocity winds may cause power outages; this could be achieved with a wind-powered electricity generator. It is also advisable to ensure a permanent supply of electrical power to the blowers of the main pipe network, i.e. the network dedicated to gas collection, because the pipes dedicated to geomembrane uplift prevention may not be fully effective if the gas collection system is not operating at the same time.

4.2 Recommendations for the Case of Exposed Geomembranes

When geomembranes are exposed, i.e. not covered with a protective layer, they are likely to be uplifted by the wind. In Section 2.3, equations are provided that give the threshold wind velocity beyond which a given geomembrane is uplifted depending on the geomembrane mass per unit area, the location of the considered portion of geomembrane in the facility, and the altitude above sea level. The large tensions generated in the uplifted geomembrane are transmitted to the anchor trenches. It is important that the anchor trenches be designed to accommodate these large tensions. The design of anchor trenches is beyond the scope of this paper. However, the method presented in this paper provides two essential types of data for the design of anchor trenches: the tension, T , in the geomembrane, i.e. the tension exerted by the geomembrane on its anchor trench; and the orientation, θ , of the tension T .

Intermediate benches or anchor trenches (Figures 7c and 7d) are very effective because they decrease the length of free geomembrane subjected to wind suction. Since wind-generated suction is larger in the upper portion of a slope than in the lower portion (see Figure 5), benches or anchor trenches should be more closely spaced in the upper portion of the slope than in the lower portion. Ideal spacings are shown in Figure 26. These spacings are such that the product of the spacing and the suction factor, λ , is a constant. A remarkable example of such a design is Barlovento reservoir, constructed in 1991-1992 in a large crater (600 m diameter) in the Canary Islands, Spain (Fayoux 1992, 1993) (Figure 27) at an altitude of 700 m. A similar design had been done by the senior author in 1977 for another crater reservoir, also in the Canary Islands, but not yet constructed. The side slope of the Barlovento reservoir is 1V:2.75H and is 30 m high. In the first phase, only the bottom and the lower 20 m of the side slope were lined, using a 1.5 mm thick PVC geomembrane reinforced with a polyester scrim on the side slope and a 1.5 mm thick unreinforced PVC geomembrane on the bottom. As seen in Figure 27, because of the spiral shape of the anchor trenches, the number of anchor trenches at a given location along the slope is either three or four, in addition to one anchor trench at the top of the lined portion of the slope and one anchor trench at the toe of the slope.

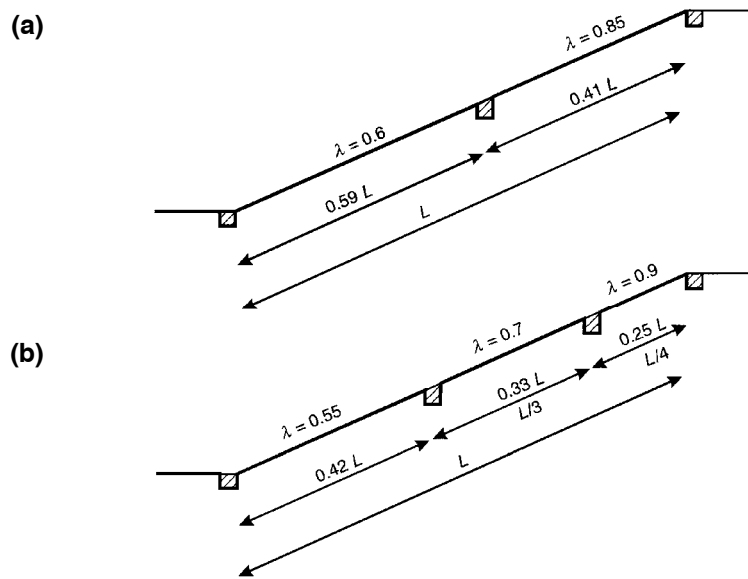


Figure 26. Ideal spacing for anchor trenches or benches on a slope: (a) two spacings; (b) three spacings.

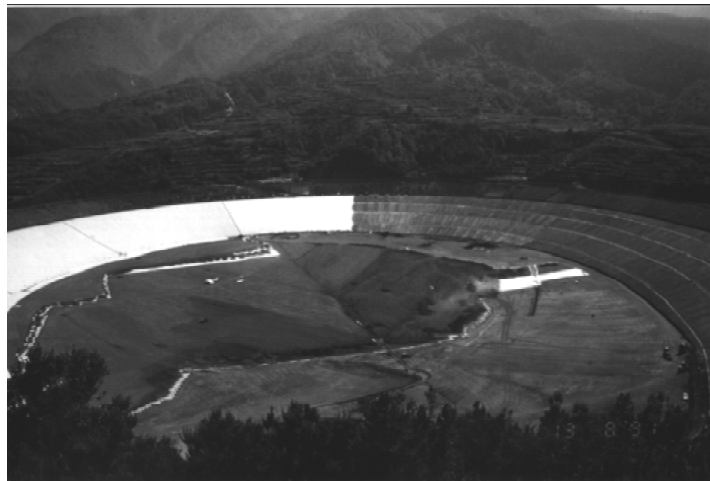


Figure 27. Barlovento reservoir in the Canary Islands (courtesy of D. Fayoux).

(Notes: Three stages of construction are seen on this photograph: 1) in the right part of the photograph, the four intermediate anchor trenches are visible; 2) in the center-right of the photograph, which appears almost identical to the right part, a layer of porous concrete has been placed on the slope and the geomembrane tabs (which are anchored in the anchor trenches and pass through the porous concrete) are visible; and 3) on the left half of the photograph, the white PVC geomembrane has been placed and seamed to the tabs. It should be noted that the anchor trenches are not horizontal, but form a spiral at the periphery because they contain a drain with a 1% slope.)

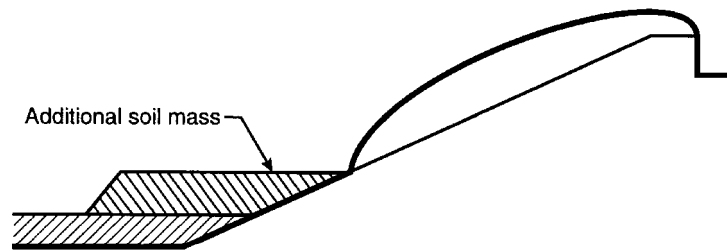


Figure 28. Additional soil mass at toe of slope to resist localized uplift of geomembrane at bottom due to tension in geomembrane on slope.

The distances measured along the slope between the anchor trenches located on the slope are, from top to bottom: 14.1 m, 15.2 m, and 18.8 m.

As indicated in Section 4.1, a relatively thin soil layer is sufficient to prevent geomembrane uplift at the bottom of a pond. However, this thin soil layer may not be sufficient as an “anchorage” to resist localized uplift due to the tension of the uplifted geomembrane at the toe of the slope. Therefore, an additional soil mass at the toe of the slope is required, as shown in Figure 28.

As indicated in Section 4.1, suction vents are generally believed to be an effective way to prevent or reduce uplift by the wind of exposed geomembranes located on a slope. Therefore, suction vents should be considered every time the slopes of a geomembrane-lined facility are expected to be exposed to high-velocity winds and cannot be covered with a protective layer for any reasons such as stability or cost. However, it is hard to find documented information on the performance of suction vents and a design method needs to be developed.

5 CONCLUSIONS

The detailed analysis of the phenomenon of uplift of geomembranes by wind presented in this paper has yielded the following results:

- The uplift effect of wind on geomembranes depends on wind velocity, altitude above sea level, and location of the geomembrane in the considered facility (e.g. the geomembrane is more likely to be uplifted if it is at the crest of a dike than on a side slope, and more likely to be uplifted on a side slope than at the bottom). Equations were provided to calculate the wind-generated suction as a function of these parameters.
- Whether or not a geomembrane will be uplifted by the wind depends on the above parameters and on the mass per unit area of the geomembrane. At a given location, the threshold wind velocity at which a geomembrane starts being uplifted is higher for a heavy geomembrane (such as a bituminous geomembrane) than for a light geomembrane (such as a polymeric geomembrane). Equations were provided to calculate threshold wind velocities.
- When a geomembrane is uplifted, its tension, strain, and deformation depend on its tensile characteristics. Equations, tables and graphical methods were provided to de-

termine the tension, strain and geometry of uplifted geomembranes as a function of wind velocity, altitude above sea level, location of the geomembrane in the considered facility, and tensile characteristics of the geomembrane. Geomembranes with a high tensile stiffness (i.e. high modulus) deform less than geomembranes with a low tensile stiffness, but they undergo a greater tension and apply a greater pullout force on anchor trenches.

- The condition of the geomembrane when uplifting begins has a significant influence on the magnitude of uplifting and the condition of the uplifted geomembrane. If a geomembrane has wrinkles when uplifting begins, it is uplifted more, but with a smaller tension than if the geomembrane has no wrinkles when uplifting begins. If a geomembrane is under tension when uplifting begins, it is uplifted less, but with a greater tension than if the geomembrane is not under tension when uplifting begins.
- Since temperature has a significant effect on the tensile characteristics of geomembranes, the effect of temperature on geomembrane uplift by wind has been analyzed. At a given location and for a given wind velocity, a given geomembrane will exhibit less strain but more tension at low temperature than at high temperature. The method presented in this paper allows the designer to quantify the effect of temperature on wind uplift. It has been shown that HDPE geomembranes resist wind uplift better at low temperature than at high temperature (i.e. the factor of safety based on allowable tension and strain is greater at low than at high temperature).
- The most effective way to prevent the wind from uplifting geomembranes is to place a protective cover on the geomembrane. Typical protective covers consist of a layer of soil or rock, concrete slabs or pavers, and bituminous revetments. A method has been provided to determine the required thickness of the protective cover. Examples presented in the paper show that a few centimeters are generally sufficient.
- Liquid stored in a pond is an effective way to prevent the wind from uplifting the geomembrane at the bottom of a pond. Equations which allow the determination of the required depth of liquid are presented in the paper.
- Sandbags scattered on the geomembrane are only efficient to prevent geomembrane uplift by low-velocity winds. The best way to use sandbags, during construction, is to place a continuous row of sandbags at the edge of the installed portion of the geomembrane to prevent the wind from getting under the geomembrane.
- Suction vents are based on a sound concept and they are believed to be effective in preventing the wind from uplifting geomembranes or in reducing the magnitude of geomembrane uplift. However, to the best of the authors' knowledge, there is no method available for the design of suction vents, and there is little information on their performance. A variation of the suction vent strategy for landfill covers is to modify the active gas collection system, if present, so that the blowers apply a small suction directly beneath the geomembrane cover to prevent uplift by wind.

The methods proposed in this paper are presented in a way that should be convenient for design engineers, i.e. with equations, tables, graphical solutions and numerous design examples. The senior author has used these methods, or previous versions of these methods, for the design of a number of geomembrane-lined structures since the early 1970s.

ACKNOWLEDGMENTS

The authors are pleased to acknowledge D. Fayoux of Groupe Solvay, Belgium, for the valuable information he provided on the Barlovento reservoir and for the photograph in Figure 27. The authors are also pleased to acknowledge B. Clark for the valuable information she provided on landfill gas collection. The authors are grateful to M.V. Khire for his review of the paper and to G. Saunders, A. Mozzar, S.M. Berdy and K. Labinaz for their assistance in the preparation of the paper. Furthermore, the senior author is pleased to acknowledge the information and support provided by P. Huot in the 1970s.

REFERENCES

- Dedrick, A.R., 1973, "Air Pressures over Reservoir, Canal, and Water Catchment Surfaces Exposed to Wind", Ph.D. Thesis, Utah State University, Logan, Utah, USA, 189 p.
- Dedrick, A.R., 1974a, "Air Pressures over Surfaces Exposed to Wind. Water Harvesting Catchments", Transactions of the ASAE, Vol. 17, No. 5, pp. 917-921.
- Dedrick, A.R., 1974b, "Aerodynamic Pressure Distributions over Reservoir, Canal, and Water Catchment Surfaces Exposed to Wind", *Proceedings of the 6th International Colloquium on Plastics in Agriculture*, Vol. 1, Buenos Aires, Argentina, September 1974, pp. 207-211.
- Dedrick, A.R., 1975, "Air Pressures over Surfaces Exposed to Wind. Reservoirs", Transactions of the ASAE, Vol. 18, No. 3, pp. 508-513.
- Fayoux, D., 1992, "Use of PVC Geomembranes for Large Irrigation Works", *Proceedings of XII Congreso Internacional de Plasticos en Agricultura*, Granada, Spain, May 1992, pp. I-43 - I-46.
- Fayoux, D., 1993, "Le Bassin de Barlovento, The Barlovento Reservoir", *Proceedings of Rencontres '93*, French Committee of Geotextiles and Geomembranes, Conference held in Tours, France, September 1993, Vol. 2, pp. 365-374. (in French and English)
- Giroud, J.P., 1977, "Conception de l'étanchéité des ouvrages hydrauliques par géomembranes", *Proceedings of the First International Symposium on Plastic and Rubber Waterproofing in Civil Engineering*, Vol. 1, Session 3, Paper 13, Liège, Belgium, June 1977, pp. III 13.1-III 13.17. (in French)
- Giroud, J.P. and Huot, P., 1977, "Conception des barrages en terre et en enrochements munis d'étanchéité par feuille mince", *Proceedings of the 11th Conference Européenne de la Commission Internationale de l'Irrigation et du Drainage, CIID*, Theme 3, Rome, Italy, May 1977, 8 p. (in French)
- Giroud, J.P., 1994, "Quantification of Geosynthetics Behavior", *Proceedings of the 5th International Conference on Geotextiles, Geomembranes and Related Products*, Vol. 4, Singapore, September 1994, pp. 1249-1273.
- Goldstein, S., 1938, "Modern Developments in Fluid Dynamics", Vol. 2, Oxford Engineering Science Series, Oxford University Press, United Kingdom, 702 p.

Soderman, K.L. and Giroud, J.P., 1995, "Relationships Between Uniaxial and Biaxial Stresses and Strains in Geosynthetics", *Geosynthetics International*, Vol. 2, No. 2, pp. 495-504.

The U.S. Standard Atmosphere, 1976, U.S. Government Printing Office, Washington, D.C., USA.

NOTATIONS

Basic SI units are given in parentheses.

A	=	area of a geomembrane (m^2)
D	=	thickness of protective layer (m)
D_{req}	=	required depth of protective layer (m)
F	=	force applied on geomembrane by uplift suction (defined in Equation 42) (kN/m)
g	=	acceleration due to gravity (m/s^2)
J	=	geomembrane tensile stiffness (N/m)
L	=	length of geomembrane subjected to suction (m)
L_{min}	=	minimum value of L (m)
L_{max}	=	maximum value of L (m)
p	=	atmospheric pressure at altitude z above sea level (Pa)
p_o	=	atmospheric pressure at sea level (Pa)
R	=	radius of circular-shaped uplifted geomembrane (m)
S	=	suction (Pa)
S_e	=	"effective suction" defined by Equation 35 (Pa)
T	=	geomembrane tension (N/m)
T_{all}	=	allowable tension (N/m)
T'_{all}	=	normalized allowable tension as defined by Equation 48 (N/m)
T_{base}	=	tension in an uplifted geomembrane for the base case where the geomembrane has no wrinkles and no tension when uplifting begins (N/m)
T_1	=	tension in an uplifted geomembrane that had wrinkles when uplifting began (N/m)
T_2	=	tension in an uplifted geomembrane that was under tension when uplifting began (N/m)
t_{GM}	=	thickness of the geomembrane (m)
u	=	geomembrane uplift (m)
V	=	wind velocity (m/s)
V_{up}	=	wind velocity that causes geomembrane uplift (m/s)

V_{upmin}	=	minimum value of V_{up} (m/s)
W	=	weight of a geomembrane (N)
z	=	altitude above sea level (m)
α	=	coefficient of thermal expansion-contraction of the geomembrane ($^{\circ}\text{C}^{-1}$)
β	=	lapse rate ($^{\circ}\text{K/m}$)
Γ	=	temperature of the geomembrane when uplift occurs ($^{\circ}\text{C}$)
Γ_{base}	=	temperature of the geomembrane when it rests on the supporting ground without wrinkles and without tension ($^{\circ}\text{C}$)
Γ_0	=	standard air temperature at sea level ($^{\circ}\text{K}$)
Δp_R	=	reference pressure variation (Pa)
ε	=	geomembrane strain (dimensionless)
ε_{all}	=	allowable strain (dimensionless)
ε_{app}	=	apparent strain of geomembrane (dimensionless)
ε_{app1}	=	apparent strain in an uplifted geomembrane that had wrinkles when uplifting began (dimensionless)
ε_{app2}	=	apparent strain in an uplifted geomembrane that was under tension when uplifting began (dimensionless)
ε_{base}	=	strain in an uplifted geomembrane for the base case where the geomembrane has no wrinkles and no tension when uplifting begins (dimensionless)
ε_T	=	thermal contraction or expansion as defined by Equation 58 (dimensionless)
θ	=	angle between the extremities of the geomembrane and the straight line passing through these extremities ($^{\circ}$)
λ	=	suction factor defined by Equation 13 (dimensionless)
μ_{GM}	=	mass per unit area of the geomembrane (kg/m^2)
μ_{GMreq}	=	mass per unit area of the geomembrane required to resist wind uplift (kg/m^2)
ρ	=	air density (kg/m^3)
ρ_{GM}	=	density of the geomembrane (kg/m^3)
ρ_o	=	air density at sea level (kg/m^3)
ρ_P	=	density of the protective layer material (kg/m^3)